Theory of unstable growth

Gene F. Mazenko
The James Franck Institute and Department of Physics, The University of Chicago, Chicago, Illinois 60637
(Received 16 April 1990)

A long-time universal fixed point for domain growth in a general nonconserved time-dependent Ginzburg-Landau model is established. Both the scaling function $F(x)$ and the growth law or scaling length $L(t)$ associated with this fixed point are shown to have universal features. The scaling function depends only on the spatial dimensionality, not on the form of the degenerate double-well potential, the lattice or continuum spatial structure, or on the initial conditions. The growth law, measured in units of the equilibrium interfacial width ξ, is found to have a universal amplitude multiplying the expected $t^{1/2}$ curvature drive time dependence. The universal amplitude in $L(t)$ is connected to the large-distance behavior of the scaling function through a nonlinear eigenvalue problem. For intermediate distances, $\xi \le R \le L$, the scaling law obeys Porod's law, $F=1-\alpha|\mathbf{R}|/L$, with $\alpha=\sqrt{2/\pi(d-1)}$, where d is the dimensionality of the system. The theory developed here is accurate for all times after an initial quench from a completely disordered state to a temperature well below the critical temperature. Comparisons with direct numerical simulations show excellent agreement at early and intermediate times. For later times various features predicted by the theory are in very good agreement with the simulations. It appears, however, that the selection process determining the amplitude of $L(t)$ is rather sensitive to finite-size effects, and a direct comparison between theory and simulation on this point requires simulations on much larger systems.

I. INTRODUCTION

There have been various indications that there is some degree of universality in the growth kinetics of ordering systems. It is known that the order-parameter structure factor satisfies a scaling relation[1,2] if all lengths are scaled by the characteristic domain size $L(t)$ in the large-time t limit. The time dependence of $L(t)$, the growth law for the system, is robust for a variety of systems. For example, the growth law for relaxational systems with a nonconserved order parameter is determined by the curvature driven diffusion[3] of domain walls and given by the Lifshitz-Cahn-Allen law $L \sim t^{1/2}$. The scaling behavior in a variety of systems has been shown[4] to be associated with a zero-temperature renormalization-group fixed point. Any universal features are therefore associated with zero- or low-temperature growth properties, and at the longest-time scales one expects a scaling function which is independent of temperature. The question arises: How universal is the zero-temperature scaling function? Simulation work[5] indicates general agreement for the shape functions for a number of different systems. Are these behaviors approximately equivalent or is there precise agreement? To answer such questions requires a theoretical treatment[6] with the capability of computing in the long-time regime.

In a recent Letter[7] a new theoretical method for treating growth kinetics problems was introduced. In this paper this approach is discussed in more detail and extended to treat a much larger class of systems. The relevance of a nonlinear eigenvalue problem in selecting a universal value for the parameter $\mu=L\dot{L}$ introduced in Ref. 7 is established. This selection mechanism fixes the value of μ in the large-time limit and leads to the conclusion, if this fixed point is physically accessible, that the associated structure factor is universal. Indeed μ and the structure factor depend only on the dimensionality of the system for the rather large class of systems studied in this paper.

While one can carry out the theory developed here in great detail and study almost every aspect of the growth process, the focus will be on those questions associated with universality. A general class of time-dependent Ginzburg-Landau (TDGL) models for a scalar order parameter ψ characterized by a potential $V(\psi)$ is defined in the next section. In Ref. 7 only the standard "ψ^4" potential was considered. In the work here the analysis is extended to the general class of symmetric potentials with quadratic minima. It is shown below that the long-time ordering kinetics for this general class of models is governed by exactly the same scaling function as for the ψ^4 case as long as the growth law is measured in units of the associated zero-temperature interfacial width ξ (which does depend on the form of the potential). In particular, the associated scaling function satisfies Porod's law[8] in the appropriate spatial regime (described in detail below) with a coefficient which is universal for this general class of potentials.

The analysis in this paper will be restricted to the simplest case of a single scalar order parameter that is not conserved (NCOP). As discussed in Ref. 7, the case of the conserved order parameter (COP) can be discussed in the same fashion as for the NCOP, but there is an intermediate time crossover from a $t^{1/4}$ to a $t^{1/3}$ behavior which complicates the analysis considerably. This COP case will therefore be discussed in a separate publication. The development in Ref. 7 has already been extended to the case of several scalar order parameters by Lai[9] who treated the case of a model appropriate for Cu_3Au. In

that case one has a set of three scalar order parameters which are coupled to the fcc structure of the lattice. The key result in his analysis is that the structure factor is anisotropic as is observed[10] in x-ray-scattering experiments.

The theoretical development discussed in this paper is a natural extension of the work by Mazenko, Valls, and Zannetti[11] (MVZ). They showed how growth kinetics problems defined in terms of Langevin equations could be expressed in terms of functional integrals. More importantly, they showed how the theory can be organized in terms of two independent fields corresponding to the ordering and equilibrating components of the order-parameter field. One can associate a characteristic length with each of these components. The characteristic domain size $L(t)$ goes with the ordering components of the order parameter and the equilibrium correlation length ξ is associated with the fluctuations of the equilibrated portion of the order-parameter field. The same basic idea is followed here. The significant difference between the development here and that in MVZ is the method used to construct the ordering component of the field. In MVZ it was assumed that the ordering component could be chosen to be Ising-like variable for all times after the quench with an evolving, time-dependent amplitude. As discussed in ref. 12, this assumption does not allow one to treat sharp interfaces. In this paper, a general method is developed for constructing the appropriate ordering component of the order-parameter field which allows a detailed analysis of the developing sharp interfaces. As discussed below, a key test that sharp interfaces are produced in the development is the natural occurrence of Porod's law in the theory.

It is worthwhile considering two heuristic arguments which lead to indicators of sharp interfaces in a theory. Consider first[13] the local order-parameter correlation function

$$S(t)=\langle \psi^2(\mathbf{R},t)\rangle \ . \tag{1.1}$$

Assume that we have a collection of large well-ordered domains of characteristic size L in which $\psi=\pm\psi_0$. These domains are separated by sharp interfaces of width ξ. We then estimate that $\psi^2\sim\psi_0^2$, over a fraction of space $[L/(L+\xi)]^d$ in d dimensions while $\psi^2\approx 0$ over a fraction of space $1-[L/(L+\xi)]^d$. This leads to the estimate

$$S(t)\approx\psi_0^2\left[\frac{L}{L+\xi}\right]^d\approx\psi_0^2\left[1-\frac{d\xi}{L(t)}+\cdots\right] \tag{1.2}$$

for $L\gg\xi$. The result that the first correction to $S=\psi_0^2$ is of $O(L^{-1})$ is not satisfied by previous first-principle theories.[6]

A second argument, due to Porod[8] and extended by Tomita,[14,15] can be expressed in very simple terms. Suppose, as a function of a coordinate x there is a sharp interface at some position x_0, then the order parameter shows the behavior

$$\psi(x)=\psi_0\mathrm{sgn}(x-x_0) \ .$$

Suppose we compute the correlation of $\psi(x)$ with $\psi(x')$ where we average over the position of the interface

$$c(x,x')\equiv\frac{1}{2L}\int_{-L}^{+L}dx_0\psi(x)\psi(x') \ ,$$

where L is a very large distance between interfaces. We easily obtain

$$c(x,x')=\psi_0^2\left[1-\frac{|x-x'|}{L}\right] \ .$$

This argument can be cleaned up and, when expressed in d dimensions, the order-parameter correlation function takes the form

$$C(\mathbf{R},t)=\psi_0^2\left[1-\frac{\alpha|\mathbf{R}|}{L}+\cdots\right] \ , \tag{1.3}$$

where α is some generally unknown coefficient. If this result is Fourier transformed over space, one obtains the usual expression of Porod's law for sharp interfaces $C(\mathbf{q},t)\sim q^{-(1+d)}$ for "large" q. In the theory developed here (1.3) is established quantitatively with explicit results for the coefficient α as a function of d.

Note that the results (1.2) and (1.3) are compatible if, as $\mathbf{R}\to 0$, the interface becomes smooth for $R\sim\xi$, the interfacial width. This tells us that Porod's law is valid only over the spatial range $\xi\ll R\ll L$. The theory developed here allows one to investigate the entire spatial regime $0\le R\sim L$ including the crossover discussed above.

Since the theory developed below is somewhat complex and introduces various auxiliary quantities, it is useful to summarize here the results of the theory which can be expressed in terms of observables and can be tested by further numerical work and, where appropriate, experiments.

(1) The theory gives an $S(t)$, defined by (1.1), in qualitative agreement with (1.2). Thus, one can use as a fundamental definition of L,

$$L(t)=\frac{\xi}{\sqrt{2}}[1-S(t)/\psi_0^2]^{-1} \ , \tag{1.4}$$

where $S(t)$ is defined by (1.1) and ξ is rigorously defined in equilibrium. The theory gives that the growth law [defined by (1.4)] has the long-time form

$$L=\sqrt{2\mu_*(d)}(2\Gamma t)^{1/2} \ , \tag{1.5}$$

where the $\mu_*(d)$ depend only on the dimensionality of the system and are given by (5.22) below and Γ is the fundamental unit of time defined by (2.1) below. In direct comparison with numerical simulations, excellent agreement between theory and "experiment" is obtained for $S(t)$ for short and intermediate times. For longer times it appears (see the discussion in Sec. VII) that the simulation values for $S(t)$ are rather sensitive to finite-size effects and the agreement is only fair.

(2) The theory predicts that the second moment

$$S_2=\langle(\nabla\psi)^2\rangle \tag{1.6}$$

behaves as L^{-1} for long times. In particular, for the ψ^4 potential $S_2L=\sqrt{2}/3=0.471$. Direct simulation of the same system gives good agreement with a value of 0.488.

(3) For short distances $R\ll L$ the theory gives a de-

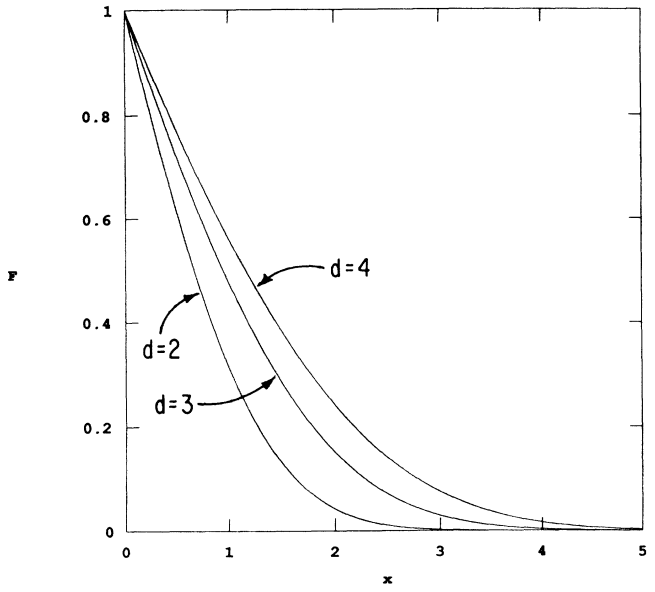

FIG. 1. Universal scaling function defined by Eq. (1.8) for $d=2$, 3, and 4 vs scaled distance $x=R/L$, where L is defined by (1.4).

tailed treatment of the average interfacial structure. We have that

$$C(R)=\psi_0^2[1-W(R)/L+\cdots], \tag{1.7}$$

where, for $R\gg\xi$, $W(R)$ is linear in $|\mathbf{R}|$, and $C(\mathbf{R},t)$ satisfies Porod's law (1.3) with $\alpha=\sqrt{2/\pi(d-1)}$. For short distances $R\sim\xi$, $W(\mathbf{R})$ is analytic in $\mathbf{R}$. Clearly the short-distance behavior of W is not universal since it probes the structure of the interface. Simulations presented below were not run to long enough times to be able to extract the coefficient in Porod's law.

(4) In the scaling regime, $R\gg\xi$, a rather simple scaling equation determining

$$C(R,t)=\psi_0^2F(\mathbf{R}/L) \tag{1.8}$$

is obtained. In the limit of small $x=R/L$, Porod's law is regained in the form described above. For large x

$$F(x)=F_0x^{(-d+\pi/2\mu)}e^{-(\mu/2)x^2}, \tag{1.9}$$

where $\mu=L\dot{L}$. This μ is the same quantity occuring in (1.5) and, of course, has the same universal values $\mu_*(d)$ in the scaling regime. $F(x)$ is determined numerically for all x for $d=2$, 3, and 4 as shown in Fig. 1. The $F(x)$ determined by direct numerical simulation is known only for modest times and the agreement with the theory is satisfactory. The long-distance behavior, however, before finite-size effects set in, are well described by (1.9) with an estimate for μ_* in good agreement with the theory.

II. STRUCTURE OF THEORY

A. Definition of problem

The system treated here is the time-dependent Ginzburg-Landau model in the presence of Gaussian noise. In terms of dimensionless length scales, the basic equation of motion satisfied by the order-parameter field $\psi(\mathbf{R},t)$ is

$$\frac{\partial\psi(\mathbf{R},t)}{\partial t}=-\Gamma\frac{\delta F}{\delta\psi(\mathbf{R},t)}+\eta(\mathbf{R},t), \tag{2.1}$$

where the Gaussian noise satisfies

$$\langle\eta(\mathbf{R},t)\eta(\mathbf{R}',t')\rangle=T\Gamma\delta(\mathbf{R}-\mathbf{R}')\delta(t-t'), \tag{2.2}$$

T is a dimensionless measure of the final temperature, and the driving effective Hamiltonian is assumed to be of the general form

$$F=\int d^dR[\tfrac{1}{2}(\nabla_R\psi)^2+V(\psi)]. \tag{2.3}$$

$V(\psi)$ is assumed to be a symmetric degenerate double-well potential with quadratic minima. A particular realization is the "λ potential"

$$V(\psi)=\tfrac{1}{4}(1-\psi^2)^2+\frac{\lambda}{6}\psi^6. \tag{2.4}$$

For $\lambda=0$ this reduces to the standard ψ^4 potential discussed in Ref. 7. A clear check on the universality of our results will be their dependence on λ. Henceforth, the ψ^4 potential will be referred to as the $\lambda=0$ potential.

The equation of motion (2.1) must be supplemented by a set of initial conditions at time $t=t_0=0$ satisfied by $\psi(\mathbf{R},t_0)=\psi_0(\mathbf{R})$. For our purposes here, where the system is assumed to be initially disordered, we assume an initial probability distribution governing ψ_0 which is Gaussian and with second moment

$$\langle\psi_0(\mathbf{R})\psi_0(\mathbf{R}')\rangle=\epsilon_I\delta(\mathbf{R}-\mathbf{R}'). \tag{2.5}$$

B. The functional-integral formulation of the problem

MVZ discussed in some detail how the Langevin equation problem defined in the last section can be transformed into a functional-integral description of the problem. This reformulation of the problem facilitates the subsequent set of transformations where the "peak" and "phonon" portions of the order-parameter field are separated. After formally replacing the averaging over the noise by a functional integration over the order-parameter field, one obtains the generating functional

$$Z[U]=\int D[\psi_0]D[\hat{\psi}]D[\psi]\times e^{-A[\psi_0,\hat{\psi},\psi]}\exp\left[\int dU(1)\psi(1)\right], \tag{2.6}$$

where $\hat{\psi}$ is the conjugate field introduced by Martin, Rose, and Siggia,[16] and one must perform functional integrals over $\hat{\psi}$, ψ, and the initial field ψ_0. The "action" A is given for the problem defined in the last section by

$$A[\hat{\psi},\psi,\psi_0]=A[\psi_0]+\int d1\{i\hat{\psi}(1)[B(1;\psi)-\delta(t_1-t_0)\psi_0(1)]\}, \tag{2.7}$$

where

$$B(1;\psi)=\Lambda(1)\psi(1)+V'[\psi(1)]\ , \tag{2.8}$$

$$\Lambda(1)=\frac{\partial}{\partial t_1}+\Gamma(-\nabla_1^2)\ , \tag{2.9}$$

and $\int d1=\int d^dR_1\int_{t_0}^{+\infty}dt_1$. To simplify things somewhat it has been assumed that the quench is to zero temperature [$T=0$ in (2.2)]. Normalizations and regularizations[17] have been chosen such that the Jacobian associated with the transformation from a functional integral over the noise to one over the field ψ is a constant. The part of the action governing the initial values of ψ is given by

$$A[\psi_0]=\tfrac{1}{2}\int d^dR_1\frac{1}{\epsilon_I}\psi_0^2(\mathbf{R}_1)\ . \tag{2.10}$$

All correlation functions among the order-parameter fields can be determined by taking derivatives of $\ln Z[U]$ with respect to the external source field $U(1)$.

C. Introduction of the peak variables

A key step in the theory is to divide the order-parameter field ψ into a peak contribution and a fluctuating component. The first step in this process is the introduction of an auxiliary field $m(\mathbf{R},t)$. If the initial function space is governed by the probability distribution

$$P[\hat{\psi},\psi,\psi_0]=e^{-A[\hat{\psi},\psi,\psi_0]}/Z_\psi\ , \tag{2.11}$$

then one must treat the enlarged space

$$P[\hat{\psi},\psi,\psi_0,m]=P_0[m]P[\hat{\psi},\psi,\psi_0]\ , \tag{2.12}$$

where it is assumed that $P_0=e^{-A[m]}$ is a normalized functional of the field m. These spaces are coupled by making the translation

$$\psi(1)=\sigma[m(1)]+\phi(1)\ , \tag{2.13}$$

where σ is a local functional of m and ϕ replaces ψ as the independent field.

After making the translation (2.13) the total "action" governing $P[\hat{\psi},\phi,\psi_0,m]$ becomes

$$A_T(\hat{\psi},\phi,\psi_0,m)=A[\psi_0]+A[m]+\int d1\,i\hat{\psi}(1)[B(1;\sigma+\phi)-\delta(t_1-t_0)\psi_0(1)]\ . \tag{2.14}$$

Inserting (2.13) in (2.8) one has

$$B(1;\sigma+\phi)=B(1;\sigma)+\Lambda(1)\phi(1)+\Gamma[V'(\sigma+\phi)-V'(\sigma)]\ . \tag{2.15}$$

Defining

$$q_0^2(1)=\left\langle\left[\frac{\partial^2}{\partial\phi^2}V(\sigma+\phi)\right]\right|_{\phi=0}\Big\rangle_0\ , \tag{2.16}$$

where the average is over $P_0[m]$, (2.15) can be rewritten as

$$B(1;\sigma+\phi)=B(1;\sigma)-i\int d2\,G_F^{-1}(12)\phi(2)+\Gamma\tilde{V}_I(1;\sigma,\phi)\ , \tag{2.17}$$

where

$$G_F^{-1}(12)=i\left[\frac{\partial}{\partial t_1}+\Gamma[-\nabla_1^2+q_0^2(1)]\right]\delta(12)\ , \tag{2.18}$$

$$\tilde{V}_I(1;\sigma,\phi)=V'[\sigma(1)+\phi(1)]-V'[\sigma(1)]-q_0^2(1)\phi(1)\ , \tag{2.19}$$

and $\delta(12)=\delta(\mathbf{R}_1-\mathbf{R}_2)\delta(t_1-t_2)$. For the simplest case of (2.4) with $\lambda=0$, $q_0^2(1)=-1+3\langle\sigma^2\rangle$ and

$$\tilde{V}_I(1;\sigma,\phi)=3(\sigma^2-\langle\sigma^2\rangle)\phi+3\sigma\phi^2+\phi^3\ . \tag{2.20}$$

Using the results (2.17) in (2.14), A_T can be separated into the sum

$$A_T(\hat{\psi},\phi,\psi_0,m)=A_0(\hat{\psi},\phi,\psi_0,m)+A_I(\hat{\psi},\phi,\psi_0,m)\ , \tag{2.21}$$

where

$$A_0(\hat{\psi},\phi,\psi_0,m)=A[\psi_0]+A[m]+\int d1\,\hat{\psi}(1)\left[iB(1;\sigma)+\int d2\,G_F^{-1}(12)\phi(2)-i\delta(t_1-t_0)\psi_0(1)\right] \tag{2.22}$$

and

$$A_I(\hat{\psi},\phi,\psi_0,m)=\int d1\,\hat{\psi}(1)i\Gamma\tilde{V}_I(1;\sigma,\phi)\ . \tag{2.23}$$

The convention will be used below that $B(1)\equiv B(1;\sigma)$.

At this stage all of the transformations are formal and without approximations. The action $A[m]$ governing the peak variable and the functional $\sigma[m(1)]$ have not yet been specified. The main requirement is that the term $A_I(\hat{\psi},\phi,\psi_0,m)$ can be treated as a "small" perturbation on the part of the action given by $A_0(\hat{\psi},\phi,\psi_0,m)$.

D. The zeroth-order theory (formal structure)

Before one can demonstrate that the perturbation A_I given by (2.23) is actually small, the zeroth-order action A_0 given by (2.22) must be analyzed. Inspection of (2.22) shows that the fields ϕ and m are coupled through the term $i\int d1\,\hat{\psi}(1)B(1)$ in the action. This coupling in the action can be eliminated by making the translation

$$\phi(1)=\zeta(1)-\int d2\,G_F(12)iB(2) \tag{2.24}$$

so that

$$A_0(\hat{\psi},\zeta,\psi_0,m)=A[\psi_0]+A[m]+\int d\hat{\psi}(1)\left[\int d2\,G_F^{-1}(12)\zeta(2)-i\delta(t_1-t_0)\psi_0(1)\right] . \tag{2.25}$$

The original fundamental field is then expressed in terms of the new fields by

$$\psi(1)=\sigma(1)-\int d2\,iG_F(12)B(2)+\zeta(1) . \tag{2.26}$$

The evaluation of the structure factor

$$C_\psi(12)=\langle\psi(1)\psi(2)\rangle \tag{2.27}$$

can be carried out at zeroth order since the fields m and ζ are uncoupled to obtain

$$C_\psi^0(12)=C(12)-i\int d\bar{2}\,G_F(2\bar{2})\langle B(\bar{2})\sigma(1)\rangle_0 -i\int d\bar{1}\,G_F(1\bar{1})\langle B(\bar{1})\sigma(2)\rangle_0 -\int d\bar{1}\,d\bar{2}\,G_F(1\bar{1})G_F(2\bar{2})\langle B(\bar{1})B(\bar{2})\rangle_0 +C_\zeta(12) . \tag{2.28}$$

The focus in the rest of the paper will be on the peak contribution

$$C(12)=\langle\sigma(1)\sigma(2)\rangle_0 .$$

The evaluation of the phonon contribution $C_\zeta(12)$, defined by

$$C_\zeta(12)=\langle\zeta(1)\zeta(2)\rangle ,$$

is described in detail by MVZ in Sec. II F with the result

$$C_\zeta(12)=-\int d\bar{1}\,G_F(1\bar{1})G_F(2\bar{1})\delta(t_1-t_0)\epsilon_I . \tag{2.29}$$

This is as far as one can go without specifying $A[m]$ and $\sigma[m]$. At this stage one can see that it is the interaction $\tilde{V}_I(1;\sigma,\zeta-iG_FB)$ which must be small. Since $\tilde{V}_I$ is constructed to be proportional to $\phi=\zeta-iG_FB$, one must require that, on average, ζ and B be small for long times. The smallness of the phonon field ζ is guaranteed at low temperatures by the formal identification of $\zeta\sim\sqrt{T}$ at long times.

The belief that one can construct $B(1;\sigma)$, (2.8) with ψ replaced by σ, to be small for long times is based on the following physical observations. If $\sigma[m]$ can be constructed to be uniform ($=\pm\psi_0$) everywhere except near interfaces, then space and time derivatives of σ are small except near interfaces and $V'(\psi_0)=0$ by construction. While $B(1;\sigma)$ is not small near an interface, the amount of interface decreases with time and one expects that averages of $B(1;\sigma)$ will decrease toward zero for large times.

E. Specification of the peak variable

1. Qualitative notions

It is time to specify in detail the construction of the peak variable $\sigma[m]$ and its associated action $A[m]$. The main ingredients in this determination are that, for long times, $\sigma[m]\approx\pm\psi_0$ except near *sharp* interfaces where σ flips sign. The idea is that $m(\mathbf{R},t)$ is a smooth field but with an amplitude that grows inexorably with time. Thus, in some region of space,

$$m(\mathbf{R},t)=\sqrt{2S_0(t)}\sin[(y-y_0)/L_0(t)]$$

and $m(\mathbf{R},t)$ has a zero in the plane perpendicular to the y direction at $y=y_0$. Suppose that

$$\sigma[m]=\psi_0\tanh m(\mathbf{R},t) .$$

Then, away from the interface, say for $y-y_0>0$, for large $S_0(t)$, $\sigma[m]=\psi_0$, while for $y-y_0<0$, $\sigma[m]=-\psi_0$. Near $y-y_0=0$, σ shows a sharp interface even though the spatial variation of m might be quite gentle for large $L_0(t)$.

A key idea here is that m serves as a type of spatial coordinate measuring the distance to an interface. Thus, when $m\to-\infty$, the system orders in the state $-\psi_0$. As m increases through zero, σ flips, and as m goes off to infinity $\sigma\to+\psi_0$. Thus, m maps out the interfacial profile of the system. Thus, one can assume, in a formal sense, that $m\sim\sqrt{S_0}\equiv\tilde{L}$ is proportional to the characteristic length L scaling the system. One can define

$$\langle m^2\rangle=S_0=L^2/\pi \tag{2.30}$$

and assume that S_0 and L increase with time. It will be shown below that this definition of L coincides with (1.4) for long times.

2. The Gaussian assumption

Consider the average $S(t)=\langle\sigma^2(m)\rangle$, where it is assumed that

$$\sigma^2(m)=\psi_0^2[1-g(m)] ,$$

where $g(m)$ vanishes as $|m|\to\infty$. Then,

$$S(t)=\psi_0^2[1-\langle g(m)\rangle_0] .$$

Assume next that the action governing the field m, $A[m]$, is quadratic and $P_0[m]$ is a Gaussian probability distribution. If $\sigma^2(m)$ and $g(m)$ depend only on the field m at a single space-time point, one obtains, using (2.30), that

$$\langle g(m)\rangle_0=\frac{\int dm\,e^{-(1/2)m^2/S_0}g(m)}{\int dm\,e^{-(1/2)m^2/S_0}} .$$

In the limit as S_0 becomes very large, the numerator of this expression is well behaved as $S_0\to\infty$ since $g(m)$ is assumed to be integrable, but the denominator goes as $\sqrt{S_0}$. Given the identification of $S_0\sim L^2$ in (2.30), one then obtains qualitative agreement between the analysis here and the sharp interface result given by (1.2).

Thus, it appears sensible to choose $P_0[m]$ to be a Gaussian probability distribution. Since $P_0[m]$ is Gaussian, it can be specified by a *single* equation governing the second moment

$$C_0(12)=\langle m(1)m(2)\rangle_0 . \tag{2.31}$$

In choosing this determining equation for C_0 one should recall the necessity of minimizing $B(1)$ and also of decoupling the variables σ and ξ. Looking at (2.28) one sees that the peak and equilibrated contributions can be decoupled by choosing $\langle B(1)\sigma(2)\rangle_0=0$. This is, of course, completely consistent with minimizing $B(1)$. In practice, $B(1)$ and $\sigma(2)$ can be uncorrelated only for $t_1>t_0$. In general, one can choose

$$\langle B(1)\sigma(2)\rangle_0=\delta(t_1-t_0)\langle\sigma(1)\sigma(2)\rangle_0 . \tag{2.32}$$

Once the dependence of σ on m is specified, (2.32) determines C_0 and the m-field statistics completely. Recalling that $B(1)$ is given by replacing ψ by σ in (2.8), one sees that (2.32) is simply the statement that $\sigma(1)$ satisfies the noiseless version of the equation of motion (2.1) *on average.*

3. *Construction of* $\sigma[m]$

Consider, finally, the specification of the peak variable $\sigma[m]$. The general results in this section are new. The main idea to keep in mind is that m serves as a coordinate which labels the interfacial profile. It is then clear that a general, nonperturbative definition of $\sigma[m]$ is given by the classical equation for a single interface

$$\frac{1}{2}\frac{d^2\sigma}{dm^2}=V'[\sigma] \tag{2.33}$$

with the boundary conditions

$$\lim_{|m|\to\infty}\frac{d\sigma}{dm}=0 . \tag{2.34}$$

This choice is general and natural. The factor of $\frac{1}{2}$ in (2.33) is chosen simply for convenience.

One can, as usual, solve (2.33) by introducing the "conserved energy," and integrating to obtain the general result

$$m=\tfrac{1}{2}\int_0^{\sigma}\frac{dx}{\sqrt{V(x)-V(\psi_0)}} , \tag{2.35}$$

where the turning points $\pm\psi_0$ are defined by $V'(\psi_0)=0$. For the $\lambda=0$ potential one has the extremum points $\psi_0=\pm1$, $V(\psi_0)=0$, and (2.35) gives $m=\tanh^{-1}\sigma$ or $m=\tanh m$ as was simply postulated in Ref. 7.

The large-m limit of $\sigma(m)$ is dominated by the contributions near the turning point. Expanding $V(x)$ for x near ψ_0, we easily integrate to obtain

$$m=\frac{1}{[2V''(\psi_0)]^{1/2}}[-\ln(\psi_0-\sigma)+\ln(\psi_0)]$$

and one obtains for large m that

$$\sigma=\psi_0-Ce^{-[2V''(\psi_0)m]^{1/2}} , \tag{2.36}$$

where C is a constant. One therefore obtains exponential decay for large m. It is this general behavior of σ which characterizes the growth kinetic class studied here.

4. *λ potential*

Consider next the potential (2.4) in (2.35) as a nontrivial generalization of the ψ^4 case. In this case the parameter λ cannot be scaled away. The first step in treating this case is to find the "critical" or turning points which satisfy $V'(\psi_0)=0$, and are given by

$$\psi_0^2=\frac{1}{2\lambda}(\sqrt{1+4\lambda}-1) . \tag{2.37}$$

For large λ, $|\psi_0|$ is pushed toward the origin. Thus, $|\psi_0|\le1$ ($|\psi_0|=1-\lambda+\cdots$ for small λ). It is then a straightforward integration using (2.4) and (2.37) in (2.35) to obtain

$$\sigma(m)=\frac{\psi_0\sqrt{1-\epsilon}\tanh\tilde{m}}{(1-\epsilon\tanh^2\tilde{m})^{1/2}} , \tag{2.38}$$

where

$$\epsilon=\psi_0^2\frac{2\lambda}{3}\frac{1}{(1+2\lambda\psi_0^2)} , \tag{2.39}$$

$$\tilde{m}=m/\xi_0 , \tag{2.40}$$

and one measure of the interfacial width is given by

$$\xi_0^{-1}=\psi_0(1+2\lambda\psi_0^2)^{1/2} . \tag{2.41}$$

Note that σ given by (2.38) has the asymptotic form (2.36) with $C=2/(1-\epsilon)$.

In subsequent sections various integrals over the interfacial profile are needed. The relevant definition of the interfacial width is given by

$$\xi=\frac{1}{\psi_0^2}\int_{-\infty}^{+\infty}dx[\psi_0^2-\sigma^2(x)]$$

$$=\xi_0\frac{2}{\sqrt{\epsilon}}\ln(1+\sqrt{\epsilon}) , \tag{2.42}$$

where the second line is for the λ potential. Also needed are the integrals

$$\kappa_n=\int_{-\infty}^{+\infty}\frac{dx}{\xi}\sigma_n^2(x)/\psi_0^2 , \tag{2.43}$$

where $\sigma_n=d^n\sigma(x)/dx^n$.

III. EVALUATION OF m AVERAGES

A. General development

While there was an attempt in the last section to motivate the choices for $A[\sigma]$ and $\sigma[m]$, one could simply start at this point with the assumptions that $P_0[m]$ is Gaussian, that $\sigma[m]$ is determined by (2.33), and that C_0 is determined by (2.32), and work out the consequences of this theory. The first step is to investigate (2.32) which, in turn, requires that one carry out the implied Gaussian averages over the fields $\sigma[m]$ and $V'[\sigma]$. As a first step, it turns out to be useful to introduce the quantities

$$\sigma_n(1)=\frac{\partial^n}{\partial m^n(1)}\sigma(1) \tag{3.1}$$

and the correlation functions

$$C_{nm}(12)=\langle\sigma_n(1)\sigma_m(2)\rangle_0\equiv\psi_0^2\tilde{C}_{mn}(12)\ . \tag{3.2}$$

Using (2.33) and (3.1) in $B(1)$, defined by (2.8) with $\psi=\sigma$, one obtains

$$B(1)=\Lambda(1)\sigma(1)+\frac{\Gamma}{2}\sigma_2(1)\ , \tag{3.3}$$

and the fundamental equation (2.32) is given by

$$\left[\frac{\partial}{\partial t_1}+\Gamma(-\nabla_1^2)\right]C(12)+\frac{\Gamma}{2}C_{20}(12)=\delta(t_1-t_2)C(12)\ , \tag{3.4}$$

where $C(12)=C_{00}(12)$.

Representing $\sigma(1)$ in (3.2) as a Fourier integral,

$$\sigma(1)=\int\frac{dk}{2\pi}\sigma_k e^{+ikm(1)}\ , \tag{3.5}$$

one has immediately that

$$C_{nm}(12)=\int\frac{dk_1}{2\pi}\frac{dk_2}{2\pi}(ik_1)^n(ik_2)^m\times\sigma_{k_1}\sigma_{k_2}\langle e^{ik_1m(1)+ik_2m(2)}\rangle_0\ . \tag{3.6}$$

Since the underlying probability distribution for the m variables is Gaussian, for arbitrary $H(1)$,

$$\left\langle\exp\left[\int d\bar{1}\,H(\bar{1})m(\bar{1})\right]\right\rangle_0=\exp\left[\tfrac{1}{2}\int d\bar{1}\,d\bar{2}H(\bar{1})H(\bar{2})C_0(\overline{12})\right]\ , \tag{3.7}$$

where it is assumed that $\langle m(1)\rangle_0=0$ and $C_0(12)$ is defined by (2.31). In the present case of interest, comparing (3.6) and (3.7),

$$H(\bar{1})=ik_1\delta(\bar{1}1)+ik_2\delta(\bar{1}2)$$

and defining

$$S_0(1)=C_0(11)\ , \tag{3.8}$$

(3.6) reduces to

$$C_{nm}(12)=\int\frac{dk_1}{2\pi}\frac{dk_2}{2\pi}(ik_1)^n(ik_2)^m\sigma_{k_1}\sigma_{k_2}\times\exp\{-\tfrac{1}{2}[k_1^2S_0(1)+k_2^2S_0(2)+2k_1k_2C_0(12)]\}\ . \tag{3.9}$$

One can immediately derive from (3.9) the very useful derivative relations

$$\frac{\partial}{\partial S_0(1)}C_{nm}(12)=\tfrac{1}{2}C_{n+2,m}(12) \tag{3.10}$$

and

$$\frac{\partial}{\partial C_0(12)}C_{nm}(12)=C_{n+1,m+1}(12)\ . \tag{3.11}$$

At equal times $S_0(1)=S_0(2)=S_0(t)$, and

$$\frac{\partial}{\partial S_0(t)}C_{nm}(\mathbf{R},t)=\tfrac{1}{2}[C_{n+2,m}(\mathbf{R},t)+C_{n,m+2}(\mathbf{R},t)]\ , \tag{3.12}$$

where $\mathbf{R}=\mathbf{R}_1-\mathbf{R}_2$.

B. Averaging theorem

1. General form

Consider next a general average of the form

$$C_g(12\cdots n)=\langle g_1(m(1))g_2(m(2))\cdots g_n(m(n))\rangle_0\ . \tag{3.13}$$

Using the Fourier representation $\hat{g}_i(k)$ for each g_i, one can carry out the associated Gaussian averages using (3.7) and obtain

$$C_g(12\cdots n)=\int\frac{dk_1}{2\pi}\frac{dk_2}{2\pi}\cdots\frac{dk_n}{2\pi}\times\hat{g}_1(k_1)\hat{g}_2(k_2)\cdots\hat{g}_n(k_n)\times\exp\left[-\tfrac{1}{2}\sum_{i,j}k_ik_jC_0(ij)\right]\ . \tag{3.14}$$

Inserting the inverse Fourier transforms one obtains

$$C_g(12\cdots n)=\int dx_1dx_2\cdots dx_ng_1(x_1)g_2(x_2)\cdots g_n(x_n)\times\Phi(x_1,x_2,\ldots,x_n)\ , \tag{3.15}$$

where

$$\Phi(x_1,x_2,\ldots,x_n)=\int\frac{dk_1}{2\pi}\frac{dk_2}{2\pi}\cdots\frac{dk_n}{2\pi}\times\exp\left[-i\sum_j^n k_jx_j\right]\times\exp\left[-\tfrac{1}{2}\sum_{i,j}k_ik_jC_0(ij)\right]\ . \tag{3.16}$$

Φ is just a multidimensional Gaussian integral which is given by[18]

$$\Phi(x_1,x_2,\ldots,x_n)=\frac{1}{(2\pi)^{n/2}}(\det C_0)^{-1/2}\times\exp\left[-\tfrac{1}{2}\sum_{i,j}x_i\Delta_{ij}x_j\right]\ , \tag{3.17}$$

where

$$\sum_k\Delta_{ik}C_0(kj)=\delta_{ij} \tag{3.18}$$

and the sum is over the *discrete* index.

2. One-point terms

In the case of a general "one-body" average ($n=1$), (3.17) gives

$$\Phi(x_1)=\frac{1}{\sqrt{2\pi S_0(1)}}e^{-(1/2)x_1^2/S_0(1)}, \tag{3.19}$$

and averages are given by (3.15) as

$$\langle g(1)\rangle=\int\frac{dx}{\sqrt{2\pi S_0(1)}}g(x)e^{-(1/2)x^2/S_0(1)}. \tag{3.20}$$

3. Two-point correlations

For correlation functions evaluated at two distinct space-time points one can evaluate (3.17) for the case of two entries and obtain

$$\det C_0=S_0(1)S_0(2)-C_0^2(12)\equiv D^{-2} \tag{3.21}$$

and

$$\Phi(x_1,x_2)=\frac{D}{2\pi}\exp\left[-\frac{D^2}{2}[x_1^2S_0(2)+x_2^2S_0(1)-2x_1x_2C_0(12)]\right]. \tag{3.22}$$

For equal times, $S_0(1)=S_0(2)=S_0(t)$, $C_0(12)=C_0(\mathbf{R},t)$, and

$$\Phi(x_1,x_2)=\frac{\gamma}{2\pi S_0}\exp\left[-\frac{1}{2}\frac{\gamma^2}{S_0}(x_1^2+x_2^2-2fx_1x_2)\right], \tag{3.23}$$

where

$$f(\mathbf{R},t)=C_0(\mathbf{R},t)/S_0(t) \tag{3.24}$$

and

$$\gamma=(1-f^2)^{-1/2}. \tag{3.25}$$

C. Large-S_0 expansions

The key to the description of the late stages of the domain growth is the assumption that $S_0(1)$ becomes large. This will be demonstrated in detail in Sec. VI. It is useful here to write down the asymptotic expressions for various quantities in the large-S_0 limit.

1. One-point quantities

In the case of the averages over quantities which depend on only a single space-time point, (3.23), the large-S_0 limit depends on whether $g(x)$ decays to zero for large x or not. If $g(x)$ does not converge to zero for large x, one can write

$$g(x)=g(\infty)+\Delta g(x), \tag{3.26}$$

and in the average over $\Delta g(x)$ one can expand $\Phi(x_1)$ in powers of S_0^{-1} to obtain

$$\langle g(1)\rangle_0=g(\infty)+\frac{1}{\sqrt{2\pi S_0(1)}}\sum_{n=0}^{\infty}\left[-\frac{1}{2S_0(1)}\right]^n\frac{1}{n!}\times\int_{-\infty}^{+\infty}dx\,x^{2n}\Delta g(x). \tag{3.27}$$

This expansion assumes that the integrals over $x^{2n}\Delta g(x)$ exist. For the particular case of the "local" order-parameter correlation function one finds

$$S(1)=\langle\sigma^2(1)\rangle_0=\psi_0^2\left[1-\frac{\xi}{\sqrt{2\pi S_0(1)}}+\cdots\right], \tag{3.28}$$

where the definition (2.42) for the interfacial width has been used. This relation connects the two expressions (1.4) and (2.30) for L.

2. Two-point quantities—$R\gg\xi$

In the regime where $R\gg\xi$, $f(\mathbf{R},t)$, defined by (3.24), is away from its value of 1 near $\mathbf{R}=0$ and, for $S_0\gg1$, $\gamma^2/S_0\ll1$. In this case one can formally expand $\Phi(x_1,x_2)$ given by (3.23) in powers of $\gamma^2/2S_0$ in (3.15) with $g_1(x_1)=\sigma_m(x_1)$ and $g_2(x_2)=\sigma_n(x_2)$ for $n+m>0$, and do the x_1 and x_2 integrations to obtain

$$\tilde{C}_{mn}(\mathbf{R},t)=\delta_{m,1}\delta_{n,1}\frac{2\gamma}{L^2}[1+O(S_0^{-1})]. \tag{3.29}$$

One can construct the leading contribution to $C=C_{00}$ by integrating the derivative result (3.11) for $n=m=0$ to obtain

$$C=\int_0^{C_0}dx\,C_{11}(S_0,x). \tag{3.30}$$

Inserting the result (3.29) into (3.30) one directly obtains that

$$C=\frac{2\psi_0^2}{\pi}\int_0^f df'(1-f'^2)^{-1/2}=2\frac{\psi_0^2}{\pi}\sin^{-1}f. \tag{3.31}$$

Given $C=C_{00}$ one can generate all the other correlation functions by differentiation. For example,

$$C_{20}=\frac{\partial}{\partial S_0}C_{00}=-\frac{2\psi_0^2}{\pi S_0}\frac{f}{(1-f^2)^{1/2}} \tag{3.32}$$

and one can obtain C_{22} by taking the derivative of C_{11} or directly using the expansion (3.29) to obtain

$$C_{22}=\frac{2\psi_0^2 f}{\pi S_0^2}\gamma^3+\cdots. \tag{3.33}$$

It is very useful to note that one can use (3.31) to express f in terms of C in C_{20} to obtain

$$C_{20}=-\frac{2}{\pi}\frac{\psi_0^2}{S_0}\tan\left[\frac{\pi}{2}\tilde{C}\right]. \tag{3.34}$$

This expression will be important in the development of Sec. V.

3. Two-point quantities: $R\sim\xi$

The expansion in the last section for large S_0 is valid away from $\mathbf{R}=0$ where it is valid to assume that $\gamma^2/2S_0\ll1$. When this inequality is not satisfied one must be more careful. Generally, for $n+m>0$, one has

$$C_{mn}(\mathbf{R},t)=\int dx_1 dx_2 \sigma_n(x_1)\sigma_m(x_2)\frac{\gamma}{2\pi S_0} \times\exp\left[-\frac{\gamma^2}{2S_0}(x_1^2+x_2^2-2x_1x_2f)\right], \quad (3.35)$$

where f is given by (3.24) and γ by (3.25). If one is in the near field $R/L \ll 1$ and $f\approx 1$ one can make progress. Define

$$b^2\equiv\frac{2S_0}{\gamma^2}=2(1+f)(S_0-C_0) \quad (3.36)$$

then, for large S_0,

$$f=1-\frac{b^2}{4S_0}+\cdots \quad (3.37)$$

and b serves as a rough measure of R, the distance separating the order-parameter fields. To lowest order in $1/S_0$, for fixed b, f can be set equal to 1 in the $2x_1x_2f$ term in the exponential in (3.35), and one obtains

$$C_{mn}(\mathbf{R},t) =\int dx_1 dx_2 \sigma_n(x_1)\sigma_m(x_2)\frac{1}{\pi b\sqrt{2S_0}}e^{-(x_1-x_2)^2/b^2}. \quad (3.38)$$

This procedure can be systematized using (3.37). We focus on (3.38) here. This quantity has the property that, as $b\to 0$, one obtains a δ function that picks out the $\mathbf{R}=0$ contribution. By changing to coordinates $r=x_1-x_2$ and $y=(x_1+x_2)/2$, (3.42) can be put into a form which emphasizes its large-b behavior. After a series of simple manipulations, (3.38) can be rewritten as

$$C_{mn}(\mathbf{R},t)=\frac{(-1)^{m+1}b^{-n-m}}{\sqrt{2S_0}\pi} \times\int_{-\infty}^{+\infty} dz\, \tilde{J}(bz)H_{n+m}(z)e^{-z^2}, \quad (3.39)$$

where

$$\tilde{J}(r)=\int_{-\infty}^{+\infty} dx\, \sigma(x)[\sigma(x)-\sigma(x+r)] \quad (3.40)$$

and the H_n are the standard Hermite polynomials. Equation (3.39) cannot be used directly to obtain C_{00}. The strategy here will be the same as in the last section. One first determines C_{11} and then integrates to obtain C_{00} using

$$C=S-\int_{C_0}^{S_0} dx\, C_{11}(S_0,x). \quad (3.41)$$

Using (3.39) for C_{11} and carrying out two integrations by parts, one easily finds that

$$C(\mathbf{R},t)=S(t)-\frac{1}{\sqrt{2S_0}}\frac{1}{\pi}\int_{-\infty}^{+\infty} dz\, \tilde{J}(bz)e^{-z^2}. \quad (3.42)$$

Notice that $\tilde{J}(r)$ can be expressed in the form

$$\tilde{J}(r)=\int_{-\infty}^{+\infty} dx[\sigma^2(x)-\psi_0^2+\psi_0^2-\sigma(x)\sigma(x+r)] =-\xi\psi_0^2+J(r), \quad (3.43)$$

and using (3.28) to evaluate S in the large-S_0 limit, one obtains the result

$$\tilde{C}(\mathbf{R},t)=1-W(b)/L, \quad (3.44)$$

where

$$W(b)=\int_{-\infty}^{+\infty}\frac{dx}{\sqrt{2\pi}}e^{-x^2}J(bx)/\psi_0^2. \quad (3.45)$$

Corrections to (3.44) are of $O(L^{-3})$. One can then evaluate C_{20} directly using (3.39) or use (3.12) and (3.44) to obtain

$$\tilde{C}_{20}=-\frac{1}{L}\frac{2}{b}\frac{\partial W}{\partial b}+O(L^{-3}). \quad (3.46)$$

One can then work out the small- and large-b limits for the various correlation functions. Starting with the expression (3.40) for $\tilde{J}$, one finds for small r that

$$\tilde{J}(r)=\frac{r^2}{2}\psi_0^2\xi\kappa_1,$$

where (2.43) has been used. Inserting this result in (3.42) one obtains for small b that

$$W=\frac{\xi}{\sqrt{2}}\left[1+\frac{\kappa_1 b^2}{4}+\cdots\right]. \quad (3.47)$$

The small-b limit for C_{20} is given, using (3.47) in (3.46), by

$$\tilde{C}_{20}(\mathbf{R},t)=\frac{-\xi}{\sqrt{2}L}\kappa_1. \quad (3.48)$$

Higher powers in b^2 bring in higher-order derivatives of σ.

In carrying out the large-b limit one must evaluate $\tilde{J}(r)$ for large r. It is not difficult to show that

$$\tilde{J}(r)=2\psi_0^2|r|+\cdots. \quad (3.49)$$

Inserting this result into (3.39) and doing the integration over the Hermite polynomials, one obtains, for $n+m>0$, that

$$\tilde{C}_{mn}(\mathbf{R},t)=\frac{\sqrt{(2/\pi)}(-1)^{n+1}}{b^{n+m-1}} \times\frac{(n+m)}{L}\frac{(n+m-2)!}{[(n+m)/2-1]!} \quad (3.50)$$

and these correlation functions fall off rapidly with inverse powers of b for large $n+m$.

Clearly, given (3.43), $J(r)$ also goes as $2\psi_0^2|r|$ for large r, and

$$W(b)=\sqrt{2/\pi}b+\cdots \quad (3.51)$$

for large b. Inserting (3.51) in (3.44) shows that $\psi_0^2-C(\mathbf{R},t)$ *grows* for large b, while

$$\tilde{C}_{2,0}(\mathbf{r},t)=-\frac{1}{L}\left[\frac{2}{\pi}\right]^{1/2}\frac{2}{b} \quad (3.52)$$

decays to zero with large values of b. These results will be crucial in Sec. V.

For the $\lambda=0$ potential one can evaluate $J(r)$ simply with the result

$$J(r)=\frac{2r}{\tanh r} \tag{3.53}$$

and

$$W(b)=2\left[\frac{2}{\pi}\right]^{1/2} b\int_0^{+\infty}\frac{dx\, xe^{-x^2}}{\tanh bx}\ . \tag{3.54}$$

It is worthwhile pointing out that the two expressions for $C(\mathbf{R},t)$ given by (3.31) and (3.44) overlap in the regime $\xi \ll R \ll L$. Since f can be written in the form (3.37), (3.31) can be expanded in powers of $b^2/4S_0$ and we obtain agreement with (3.44) in the regime $L \gg R \gg \xi$.

IV. EQUATIONS OF MOTION

A. General equations of motion

Armed with the results of the last section and the basic equation of motion (3.4), one can proceed to the determining equation for $S_0(1)$ and $C_0(12)$ and, in turn, the $C_{mn}(12)$. The main ingredients in the analysis, besides (3.4), are the derivative relations (3.10) and (3.11). One immediately finds that

$$\begin{aligned}\frac{\partial}{\partial t_1}C_{mn}(12)&=\frac{\partial C_{mn}(12)}{\partial C_0(12)}\frac{\partial}{\partial t_1}C_0(12)\\&\quad+\frac{\partial C_{mn}(12)}{\partial S_0(1)}\frac{\partial}{\partial t_1}S_0(1)\\&=C_{m+1,n+1}(12)\frac{\partial}{\partial t_1}C_0(12)\\&\quad+\tfrac{1}{2}C_{m+2,n}(12)\frac{\partial S_0(1)}{\partial t_1}\ ,\end{aligned} \tag{4.1}$$

$$\begin{aligned}\nabla_1 C_{mn}(12)&=\frac{\partial C_{mn}(12)}{\partial C_0(12)}\nabla_1 C_0(12)\\&=C_{m+1,n+1}(12)\nabla_1 C_0(12)\ ,\end{aligned} \tag{4.2}$$

and

$$\begin{aligned}\nabla_1^2 C_{mn}(12)&=C_{m+2,n+2}(12)[\nabla_1 C_0(12)]^2\\&\quad+C_{m+1,n+1}(12)\nabla_1^2 C_0(12)\ .\end{aligned} \tag{4.3}$$

The $C_{mn}(12)$ therefore satisfy (for t_1 and $t_2>t_0$)

$$\begin{aligned}\Lambda(1)C_{mn}(12)&=C_{m+1,n+1}(12)\Lambda(1)C_0(12)\\&\quad+\tfrac{1}{2}C_{m+2,n}(12)\frac{\partial S_0(1)}{\partial t_1}\\&\quad-\Gamma C_{m+2,n+2}(12)[\nabla_1 C_0(12)]^2\ .\end{aligned} \tag{4.4}$$

For the particular case of $m=n=0$ one has, comparing (4.4) and (3.4), for t_1 and $t_2>t_0$,

$$C_{11}(12)\Lambda(1)C_0(12)+\tfrac{1}{2}C_{20}(12)\frac{\partial S_0(1)}{\partial t_1}-\Gamma C_{22}(12)[\nabla_1 C_0(12)]^2=-\frac{\Gamma}{2}C_{20}(12)\ . \tag{4.5}$$

Since the $C_{nm}(12)$ are functionals of $C_0(12)$ and $S_0(1)$, (4.5) becomes the fundamental equation determining $C_0(12)$ and $S_0(1)$. In Sec. VI it is shown how one can numerically solve (4.5) and establish the general picture developed previously built on the idea that S_0 increases with time without bound. Using the basic equation (4.5) one can rewrite the general equation for C_{mn}, (4.4), in the form

$$\Lambda(1)C_{mn}(12)+\frac{\Gamma}{2}C_{m+2,n}(12)=\left[\frac{1}{2}\frac{S_0(1)}{\partial t_1}+\Gamma\right]\Xi_{mn}(12)+\tilde{\Xi}_{mn}(12)\Gamma[\nabla_1 C_0(12)]^2\ , \tag{4.6}$$

where

$$\begin{aligned}\Xi_{mn}(12)&=C_{m+2,n}(12)\\&\quad-C_{m+1,n+1}(12)\frac{1}{C_{11}(12)}C_{20}(12)\ ,\end{aligned} \tag{4.7}$$

$$\begin{aligned}\tilde{\Xi}_{mn}(12)&=C_{m+1,n+1}(12)\frac{1}{C_{11}(12)}C_{22}(12)\\&\quad-C_{m+2,n+2}(12)\ .\end{aligned} \tag{4.8}$$

As a nontrivial example of the use of these higher-order equations of motion, consider the quantity $\langle B(1)B(2)\rangle_0$ which appears in the zeroth-order structure factor given by (2.28). One has immediately from the definition (3.3) of $B(2)$ and (2.32), for t_1 and $t_2>t_0$, that

$$C_B(12)=\langle B(1)B(2)\rangle_0=\frac{\Gamma}{2}\langle B(1)\sigma_2(2)\rangle_0\ . \tag{4.9}$$

One can then obtain an equation of motion for $C_{02}(12)$ by setting $n=0$ and $m=2$ in (4.6). Using this result in (4.9) leads to the result

$$\begin{aligned}C_B(12)&=\frac{\Gamma}{2}\left[\frac{1}{2}\frac{\partial S_0(1)}{\partial t_1}+\Gamma\right]\Xi_{02}(12)\\&\quad+\frac{\Gamma^2}{2}\tilde{\Xi}_{02}(12)[\nabla_1 C_0(12)]^2\ .\end{aligned} \tag{4.10}$$

Therefore, if the corrections to the peak contribution in (2.28) are to be small, Ξ_{02} and $\tilde{\Xi}_{02}$ must be small.

Using techniques already developed, it is straightfor-

ward to show, in the limit of large S_0, that, near $\mathbf{R}=0$, $\Xi_{02}(0)\sim 0(L^{-3})$, while for R away from zero, $\Xi_{02}(\mathbf{R})\sim 0(L^{-4})$. Similarly for $\mathbf{R}=0$, $\tilde{\Xi}_{02}(0)\sim 0(L^{-1})$, while away from $\mathbf{R}=0$, $\tilde{\Xi}_{02}(\mathbf{R})\sim 0(L^{-6})$. While $\tilde{\Xi}_{02}(0)\sim 1/L$ for $\mathbf{R}$ near zero, $(\nabla_1 C_0)^2$ vanishes as R^2 as $R\to 0$. Thus, for $R=0$, $C_B(0)\sim 1/L^3$, while for $R\gg 1$, $C_B(R)\sim 1/L^4$ and one can conclude that this quantity is very small for late times and does not contribute to the scaling behavior.

The role of perturbative corrections to the peak contribution has been investigated in some detail. The results are that there are no low-order corrections to the scaling results. The nonzero temperature corrections are of the same form as found in Sec. III D of MVZ. The focus during the rest of the paper is on the contributions to the structure factor from the peak contribution. It is therefore assumed that, for long times, $C_\psi(\mathbf{R},t)=C(\mathbf{R},t)$.

B. Determination of $C_0(\mathbf{R},t)$

The entire premise of this theory is that C_0 and, in particular, S_0 grow with time in an unbounded fashion. To establish this result (4.5) must be solved as an initial value problem for equal times ($t_1=t_2=t>t_0$). For $R\neq 0$, (4.5) can be put in the form

$$\frac{\partial C_0(\mathbf{R})}{\partial t}=-\frac{\partial S_0}{\partial t}\frac{C_{20}(\mathbf{R})}{C_{11}(\mathbf{R})}-\frac{1}{C_{11}(\mathbf{R})}2\Gamma[\tfrac{1}{2}C_{20}(\mathbf{R})-\nabla_R^2 C(\mathbf{R})]\ , \tag{4.11}$$

while for $R=0$ one must solve

$$[C_{11}(0)+C_{20}(0)]\frac{\partial S_0}{\partial t}=2\Gamma[-\tfrac{1}{2}C_{20}(0)-S_2]\ , \tag{4.12}$$

where S_2 is defined by (1.6) with ψ replaced by σ. Equations (4.11) and (4.12) are supplemented by the initial condition

$$C(\mathbf{R},t=0)=\delta_{\mathbf{R},0}\epsilon_I\ . \tag{4.13}$$

Clearly, since $C(S_0,C_0=0)=0$, this requires

$$C_0(\mathbf{R},t=0)=\delta_{\mathbf{R},0}S_0(0)$$

and gives the equation $S[S_0(0)]=\epsilon_I$ which must be solved to obtain $S_0(0)$ in terms of ϵ_I.

In order to proceed one needs to know C, C_{11}, and C_{20} explicitly as functions of C_0 (and S_0) and then integrate (4.11) and (4.12) forward in time. Unfortunately, these quantities are generally only known as double integrals at each time step (for all $\mathbf{R}$). One must therefore develop analytic representations for these quantities (interpolation formulas) which one can check once and for all with the double integrals. The interpolation formulas used below are for the $\lambda=0$ potential and are given by

$$C=\frac{L_0^3}{L_1}\sin^{-1}\left[\frac{L_1C_0}{L_0}\right]\ , \tag{4.14}$$

$$C_{11}=\frac{L_0^2}{(1-L_1^2C_0^2/L_0^2)^{1/2}}\ , \tag{4.15}$$

and

$$C_{20}=-\frac{L_0L_1C_0}{(1-L_2C_0^2/3L_0)^{1/2}}\ , \tag{4.16}$$

where the one-dimensional integrals L_n are defined by

$$L_n(S_0)=(-2)^n\frac{\partial^n}{\partial S_0^n}\langle\sigma_1\rangle\ . \tag{4.17}$$

These interpolation formulas satisfy the first two terms in the exact expansion in powers of C_0 [which follow from (3.9)]. Using the large-S_0 results

$$L_n(S_0)=\left[\frac{2}{\pi S_0}\right]^{1/2}\frac{(2n)!}{n!}\frac{1}{(2S_0)^n}+\cdots\ , \tag{4.18}$$

it is easy to show they also reproduce the exact large-S_0 results given in Sec. III.

Finally one needs practical expressions for the L_n as functions of S_0 and for the $\mathbf{R}=0$ components of C, C_{11}, and C_{20}. It was found that the following interpolation formulas, which are exact in the large- and small-S_0 limits, give excellent fits to the numerically determined functions over the entire S_0 range, $0\le S_0<\infty$.

$$S=1-L_0\ , \tag{4.19}$$

$$L_0=(1+b_1S_0+b_2S_0^2)/(1+b_3S_0+b_2S_0^2\sqrt{S_0\pi/2})\ , \tag{4.20}$$

where $b_1=-1.512$, $b_2=3.4$, $b_3=-0.4941$;

$$L_1=2/(1+8S_0+b_1S_0^2+2\pi S_0^3)^{1/2}\ , \tag{4.21}$$

where $b_1=14.89$;

$$L_2=16/(1+17S_0+b_1S_0^2+b_2S_0^3+b_3S_0^4+\pi 128S_0^5/9)^{1/2}\ , \tag{4.22}$$

where $b_1=98.42$, $b_2=189$, $b_3=201.3$;

$$C_{11}(0)=(1+b_1S_0+b_2S_0^2)/(1+b_3S_0+1.5b_2S_0^2\sqrt{\pi S_0/2})\ , \tag{4.23}$$

where $b_1=-1.274$, $b_2=8.657$, $b_3=0.7797$;

$$C_{20}(0)=-2S_0/[(1+10S_0+b_1S_0^2+9\pi S_0^3/2]^{1/2}\ , \tag{4.24}$$

where $b_1=25.14$. The interpolation formulas (4.14)–(4.16), when checked against the direct numerical integration of the associated double integrals, are accurate to better than one-half of a percent over the entire $C_0\le S_0$ domain.

V. ANALYTIC RESULTS

A. Long-time, short-distance properties

1. General development

The long-time $L\gg 1$ and short-distance $R\ll L$ behavior of the theory is analyzed in this section. It was shown

in Sec. III that, for these conditions, the correlation functions $\tilde{C}$ and $\tilde{C}_{20}$ are given by (3.44) and (3.46), respectively. The corrections to these expressions are of $O(L^{-3})$. If these expressions are inserted into the fundamental equation (3.4) evaluated at equal times $t_1=t_2=t$, $t>t_0$, and with $\Gamma=\frac{1}{2}$, one obtains

$$\frac{\partial C}{\partial t}=-\tfrac{1}{2}C_{20}+\nabla_R^2 C \ . \tag{5.1}$$

One sees immediately that, to lowest order in powers of L^{-1}, one can drop the left-hand side and obtain, to $O(1/L)$,

$$\frac{1}{b}\frac{\partial W(b)}{\partial b}=\nabla^2 W(b) \ . \tag{5.2}$$

Since this equation is independent of time one can conclude that in the long-time $L\gg 1$ and short-distance limit $R\ll L$, b approaches a time-independent limit. This is the first indication of a long-time fixed point in this problem. Thus, to leading order in L^{-1}, C takes the form (3.44) with $W=W(\mathbf{R})$. Similarly, from (3.37), one has that $f=1-\pi b^2/4L^2+\cdots$ and therefore $C(\mathbf{R})$ and $C_0(\mathbf{R})$ are determined for $R\ll L$ by the solution of (5.2) and (3.45) for b and $W(b)$.

2. $R\ll\xi$

Consider first (5.2) in the ultrashort-distance limit $\mathbf{R}\to 0$ where $b\to 0$. In this limit it is convenient to express the results in terms of the second moment of C and C_{20} and identify as $L\to\infty$ and $\mathbf{R}\to 0$,

$$\tilde{S}_2=-\tfrac{1}{2}\tilde{C}_{20}(\mathbf{R}=0) \ . \tag{5.3}$$

Using the large-S_0 limit of $\tilde{C}_{20}(0)$, which follows from (3.27), one obtains

$$\tilde{S}_2=\frac{1}{2}\frac{\xi\kappa_1}{\sqrt{2\pi S_0}} \ . \tag{5.4}$$

For the $\lambda=0$ potential one can easily evaluate κ_1 to obtain $S_2=\sqrt{2}/3L$, and one obtains the firm prediction for the product of observables $LS_2=\sqrt{2}/3=0.471\cdots$.

More generally one can determine $b(\mathbf{R})$ for small R by using the result (3.47) for $b^2\ll 1$ in (5.2) to obtain

$$\nabla^2 b^2=2 \tag{5.5}$$

which has the solution as $R\to 0$

$$b^2=\frac{R^2}{d} \ . \tag{5.6}$$

This simple result has the consequences that

$$f(\mathbf{R},t)=1-\frac{R^2}{4dS_0(t)}+\cdots \ , \tag{5.7}$$

$$W(b)=\frac{\xi}{\sqrt{2}}\left[1+\frac{R^2\kappa_1}{4d}+\cdots\right] , \tag{5.8}$$

and $\tilde{C}$ is given by (3.44).

3. $\xi\ll R\ll L$

In this limit b is large and, using (3.51) in (5.2), one obtains

$$\frac{1}{b}=\nabla^2 b \ . \tag{5.9}$$

In the large-R regime where (5.9) is valid one easily obtains the solution

$$b=R\left[\frac{1}{\sqrt{d-1}}+\frac{1}{R^{d/2}}[f_1\cos(\gamma\ln R+\phi_1)]+\cdots\right] , \tag{5.10}$$

where

$$\gamma=\tfrac{1}{2}(8d-8-d^2)^{1/2}=\begin{cases}1, & d=2\\ \sqrt{7/2}, & d=3\end{cases} , \tag{5.11}$$

and f_1 and ϕ_1 are numbers which can be determined by numerically solving (5.9). In particular, for $d=2$, $f_1=0.56$, $\phi_1=1.19$, while for $d=3$, $f_1=0.41$, $\phi_1=0.008$. If one goes to higher order in $1/R$ or works in dimension $d\geq 4$, then higher-order terms in $1/b$ must be kept from the expansion of W in powers of b^{-1}.

Note that (5.10), when put back into (3.51), gives (1.7). Using (5.10) back in (3.37) one obtains

$$C_0(\mathbf{R})=S_0-\frac{R^2}{4(d-1)}+\cdots \ . \tag{5.12}$$

Note that $b\sim C_0-S_0\sim R^2$ for both large and small R but the coefficient of R^2 has the value $1/4d$ as $\mathbf{R}\to 0$ but $1/[4(d-1)]$ as $\mathbf{R}\to\infty$. One can also numerically determine $(b^2/R)^2$ in the intermediate regime.

4. *Time dependence*

At $O(1/L)$ the fundamental equation (5.1) generates a fixed-point solution which is independent of the details of the driving dynamics. In particular, one obtains the same results for a COP or an NCOP. Thus, one need only assume that S_0 becomes large as $t\to\infty$. Looking at the equation satisfied by S_0 one has

$$[C_{11}(0)+C_{20}(0)]\frac{\partial S_0(t)}{\partial t}=[-\tfrac{1}{2}C_{20}(0)-S_2] \ . \tag{5.13}$$

Focusing on the left-hand side one has, for the case of large S_0, that

$$C_{11}(0)+C_{20}(0)=\frac{\partial S}{\partial S_0}=\frac{\psi_0^2\xi}{2S_0\sqrt{2\pi S_0}} \tag{5.14}$$

plus higher-order corrections. Since $\dot{S}_0<\infty$, as $S_0\to\infty$ one sees that the left-hand side of (5.13) is of order $S_0^{-3/2}\dot{S}_0$. It was shown in Sec. V A 1 that the right-hand side of (5.13) vanishes to $O(L^{-1})$ which is just a restatement of (5.3). Thus, one is able to determine $b(\mathbf{R})$ independent of the particular time dependence of $S_0(1)$. If the right-hand side of (5.13) is evaluated to $O(S_0^{-3/2})$, one must keep the next order correction to (3.37) of $O(S_0^{-2})$ which introduces another unknown function

$b^{(2)}(\mathbf{R})$ analogous to $b(\mathbf{R})$. In that case, (5.13) reduces to an equation relating the unknown constant $\dot{S}_0$ and $b^{(2)}(\mathbf{R})$. This tells one that $S_0 \sim t$ for long times and one recovers the Lifshitz-Cahn-Allen[3] results $L \sim t^{1/2}$. While the same approach used to determine $b(\mathbf{R})$ can be used to evaluate $b^{(2)}(\mathbf{R})$, one finds that it is a function of $\dot{S}_0$. Thus, the number $\dot{S}_0$ remains undetermined. Understanding why this is so will emerge in the next section.

B. Scaling regime

1. Scaling equation

Consider again the fundamental equation of motion (5.1). It was shown in Sec. III for $R \gg \xi$ and $L \gg \xi$ that C_{20} can be expressed in terms of C using (3.34). Inserting (3.34) into (5.1) one obtains

$$\frac{\partial \tilde{C}}{\partial t} = \frac{1}{L^2} \tan\left[\frac{\pi}{2}\tilde{C}\right] + \nabla^2 \tilde{C} , \tag{5.15}$$

where, for large times, L is given by (1.4).

Equation (5.15) is very interesting since it directly admits a scaling solution. Assume a solution of the form (1.9). If $\mathbf{x} = \mathbf{R}/L$, then

$$\frac{\partial}{\partial t} F(\mathbf{x}) = \nabla_x F(\mathbf{x}) \cdot \frac{\partial \mathbf{x}}{\partial t} = -\frac{\mu}{L^2} \mathbf{x} \cdot \nabla_x F(\mathbf{x}) , \tag{5.16}$$

where the parameter

$$\mu = L\frac{dL}{dt} = \frac{1}{2}\frac{dL^2}{dt} = \frac{\pi}{2}\dot{S}_0 \tag{5.17}$$

can be taken to be a constant since $L \sim t^{1/2}$. Using (1.8) and (5.16) in (5.15) one arrives at the fundamental scaling equation

$$-\mu \mathbf{x} \cdot \nabla_x F(\mathbf{x}) = \tan\left[\frac{\pi}{2}F\right] + \nabla_x^2 F . \tag{5.18}$$

2. Small-x limit

Equation (5.18) can be solved analytically in the small- and large-x limits. The key point in the small-x expansion is that, for small x, $F = 1 - (2/\pi)g$, where g is small and $\tan[(\pi/2)F] \sim 1/g$ blows us as g^{-1} as $g \to 0$. One then obtains, after a straightforward calculation (assuming the system is isotropic),

$$F(x) = 1 - \left[\frac{2}{\pi(d-1)}\right]^{1/2} x \left[1 - \frac{(\mu + \pi/6)x^2}{2(2d+1)} + \cdots\right] . \tag{5.19}$$

Note that the leading term, Porod's law, agrees with the results (3.44), (3.51), and (5.10) in the regime $\xi \ll R \ll L$.

3. Large-x limit

In the large-x limit, F becomes small, one can replace

$$\tan[(\pi/2)F] \approx \frac{\pi}{2}F$$

in (5.18), and one must consider the linear equation

$$-\mu x \frac{\partial F}{\partial x} = \frac{\pi}{2}F + F'' + \frac{(d-1)}{x}F' . \tag{5.20}$$

One can then find solutions to (5.20) of the form $F = F_0 x^{-\nu} e^{-Ax^\gamma}$ with $\gamma \geq 0$ and directly obtains two solutions. The first solution has $\gamma = 2$, $A = \mu/2$, and $\nu = d - (\pi/2\mu)$ and leads to a Gaussian decay of the structure factor for large x. The second solution has $\gamma = 0$ and $\nu = \pi/2\mu$. This leads to a power-law decay at long distances.

Note, however, for $2\mu d > \pi$, the power-law behavior leads to a nonintegrable structure factor. Since the integral of the structure factor is just the $q = 0$ component of Fourier transform of the structure factor, we know that this must be finite for any finite time. Indeed, for any finite time after the quench,

$$C(\mathbf{q}=0,t) = \int d^d R\, C(\mathbf{R}) = L^d(t)\psi_0^2 \int d^d x F(\mathbf{x})$$

is assumed to be well behaved. That μ falls into the range $\mu > \pi/2d$ comes from the realization that $\dot{S}_0 \approx S_0$ for early times and one expects μ to grow as $(\pi/2)S_0$. Once μ is larger than $\pi/2d$, the system will pick out the Gaussian solution. In Sec. VI it is shown that the Gaussian solution is unambiguously selected by the direct numerical solution of (4.11).

4. Determination of μ: A nonlinear eigenvalue problem

From the analysis of the small-x behavior of F, one knows that $F(0) = 1$ and $F'(0) = -\sqrt{2/\pi(d-1)}$. Therefore, one can treat (5.20) as a standard second-order differential equation and, given $F(0)$ and $F'(0)$, integrate it out from the origin. From the large-x analysis one has that F must match onto

$$F_A = F_0 x^{(d-\pi/2\mu)} e^{-(\mu/2)x^2} + F_1 x^{-\pi/2\mu} . \tag{5.21}$$

But as explained above, for the band of μ values of interest, the term proportional to F_1 is nonintegrable and unphysical. Therefore, the branch of F determined by $F(0)$ and $F'(0)$ must match onto F_A with $F_1 = 0$. Clearly this reduces to a nonlinear eigenvalue problem where μ must be selected to give $F_1 = 0$. Thus problem can be solved relatively simply numerically and one obtains the selected values

$$\mu_* = \begin{cases} 1.104\ldots, & d=2 \\ 0.5917\ldots, & d=3 \\ 0.4144\ldots, & d=4 \end{cases} . \tag{5.22}$$

This result has far-ranging implications. If the only acceptable solution to (5.20) is for a selected set of $\mu = \mu_*(d)$, then the resulting scaling function is *universal*. This universal scaling function $F(x)$ is shown in Fig. 1 for $d = 2$, 3, and 4. This has the further implications that $\dot{S}_0, L$ and $1 - \tilde{S}$ are completely determined by this result for long times. One has, for example,

$$\tilde{S} = 1 - (\mu_* 2\Gamma t)^{-1/2} + \cdots . \tag{5.23}$$

A very interesting consequence of this result is that the behavior of the $C(\mathbf{R},t)$ at $\mathbf{R}=0$ given by (5.23) is determined by asymptotically matching to the long-distance behavior.

These results raise some interesting and difficult questions about boundary and finite-size effects. The asymptotic matching necessary to select the value of μ requires going to large values of $x=R/L$. Clearly, for $L \gg \xi$, this may require going to very large values of R. For finite-size systems with periodic boundary conditions one eventually leaves the regime where $F(x_{\max})$ is small and it is difficult to guess the selection mechanism in this case. For finite-size systems the integrability is guaranteed and the selected μ_* may be chosen differently (or not at all).

VI. NUMERICAL ANALYSIS OF BASIC EQUATIONS OF MOTION

A. Preliminaries

The results of the direct numerical solution of the fundamental set of equations (4.11) and (4.12) are presented in this section for the $\lambda=0$ potential. The first system studied is defined on a two-dimensional square lattice using the interpolation equations for $C(\mathbf{R})$, $C_{11}(\mathbf{R})$, and $C_{20}(\mathbf{R})$ given by (4.14), (4.15), and (4.16). These must be supplemented by the interpolation equations for the one-point quantities L_n, S, $C_{11}(0)$, $C_{20}(0)$, etc., also given in Sec. IV B. When implementing a numerical solution there are various practical questions one must answer. The first concerns the size of the system and the boundary conditions. Since these numerical results will be compared with simulations carried out on lattices with periodic boundary conditions, it is clear that periodic boundary conditions should be used here. The Laplacian on the square lattice is given by

$$\nabla^2 f(\mathbf{R}) = \sum_{\alpha} [f(\mathbf{R}+\delta_a)-f(\mathbf{R})] , \tag{6.1}$$

where a labels the vectors δ_a connecting $\mathbf{R}$ to its four nearest neighbors. These results for this system will be referred to as the n2fl calculation (*nonconserved, two-*dimension system, using the *full* set of equations, on a *lattice*) to distinguish it from other calculations described below.

The equations of motion (4.11) and (4.12) were solved using a straightforward time-step algorithm. It is found that there is a numerical instability in the simplest numerical analysis of these equations if the time step is chosen too large. It was found that for a time step $\Delta t=0.01$ there is no such instability for the time range of interest.

The role of finite-size effects were investigated in some detail. The main result is that finite-size effects tend to make the order grow faster and go to a final value of $S<1$. Thus, S, L, and S_0 hit a final fixed value while S_2 develops oscillations.

Most of the calculations are for systems of size $N\times N$ where $N=100$. In the time regime $0<t<400$ it was found that there is *no* significant (or visible) change from the $N=60$ results for the quantities S, S_2, or S_0.

TABLE I. Numerical fits of theory to (6.2). The various calculations n2fl, etc., are defined in the text.

	$S_0^{(0)}$	$S_0^{(1)}$
n2fl	−5.78	0.761
n2fi	−5.87	0.758
n3fi	0.237	0.384

B. Time dependence

The basic picture presented earlier is confirmed by the direct numerical solution of the basic equations of motion. Most importantly, as shown in Fig. 2 for $N=100$, $\Delta t=0.01$, and $S(0)=\frac{1}{3}$, S_0 grows monotonically with time. Indeed one sees that S_0 is linear with time after a rather short "waiting time." An excellent fit is given by the form

$$S_0 = S_0^{(1)} t + S_0^{(0)} , \tag{6.2}$$

where $S_0^{(1)}$ and $S_0^{(0)}$ are given in Table I. According to the analytic work in the last section

$$\mu_* = \frac{\pi}{2}\dot{S}_0 = \frac{\pi}{2} S_0^{(1)} .$$

Using the value for $S_0^{(1)}$ from Table I we obtain a value of $\mu_*=1.195$ in fair agreement with the theoretical result $\mu_*=1.104$.

Turning to the direct observables S is shown in Fig. 3 for the same set of parameters. We see that it properly orders by approaching the value of 1 as $t\to\infty$. The

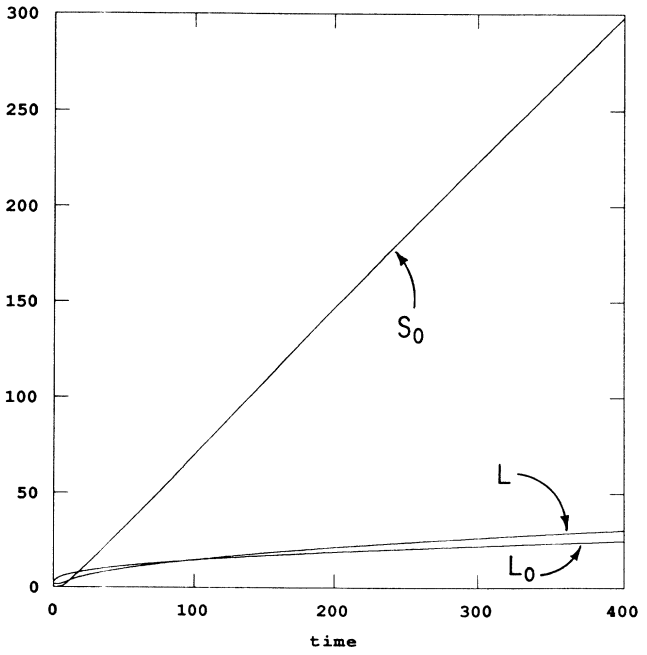

FIG. 2. S_0 vs time for the n2fl calculation defined in Sec. VI. Also plotted are L [defined by (1.4)] and L_0, the half width at half maximum, for n2fl.

TABLE II. Numerical fits of theory to (6.3).

	$L^{(0)}$	$L^{(1/2)}$	$L^{(-1/2)}$
n2fl	1.12	1.51	−13.3
n2sl	1.18	1.50	−12.7
n2fi	0.65	1.52	−10.0
n2si	1.34	1.49	−13.6
n3fi	0.871	1.08	−6.55
n3si	0.678	1.08	−4.99

growth law L, defined by (1.4) with $\psi_0=1$ and $\xi=2$ for the $\lambda=0$ potential, is plotted in Fig. 2. L is fitted to the form

$$L=L^{(1/2)}t^{1/2}+L^{(0)}+L^{(-1/2)}t^{-1/2} \tag{6.3}$$

with the parameters given in Table II. A more refined treatment involves the quantity μ defined by (5.17). Since the $t^{1/2}$ behavior of L is not in question, it is convenient to analyze μ in the form $\mu=\frac{1}{2}L^2/t$. μ is shown in Fig. 3, and fit to the form

$$\mu=\mu^{(0)}+\mu^{(-1/2)}t^{-1/2}+\mu^{(-1)}t^{-1} \tag{6.4}$$

with the parameters given in Table III. The value $\mu_*(\infty)=\mu^{(0)}=1.14$ in good agreement with the analytical value $\mu_*=1.104$. Since $\mu^{(-1)}=-16.1$ there is a relatively slow transient in the problem. As discussed in Sec. V A 2, the quantity LS_2 should approach a constant. L and S_2 were numerically determined separately and their product fit to the form

$$A=LS_2=A^{(0)}+A^{(-1/2)}t^{-1/2}+A^{(-1)}t^{-1} \tag{6.5}$$

over the time range $100\le t\le 400$ with coefficients are given in Table IV. In particular, $A^{(0)}=0.471$ in good agreement with the analytic result.

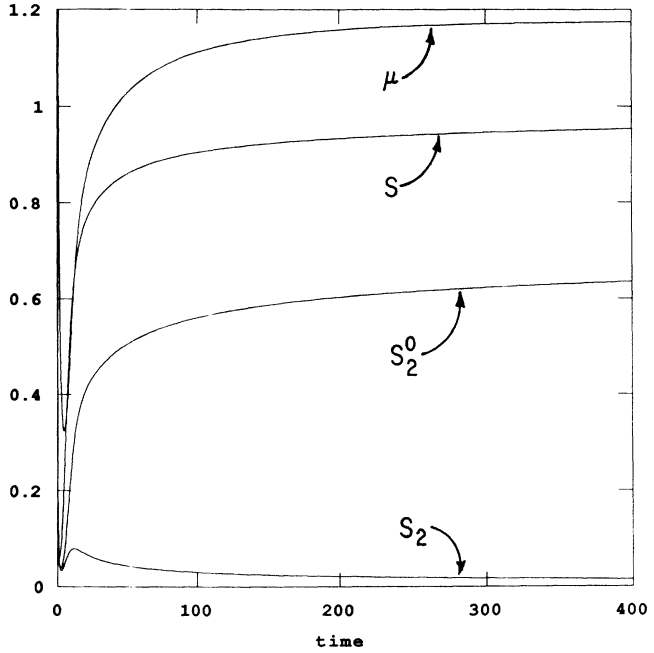

FIG. 3. Ranging from the top of the curve to the bottom $\mu=\frac{1}{2}L^2t$, S [defined by (1.1)], S_2^0, and S_2 [defined by (1.6)] are plotted for the calculation n2fl.

C. Spatial dependence

The spatial structure of the n2fl system has also been studied. The scaled structure factor $\tilde{C}(\mathbf{R},t)$ is plotted as a function of the scaled distance R/L in Fig. 4 for various times after the quench. One clearly sees the development of scaling. For larger x, $F(x)$ seems a bit more converged than for small x. A fit of $F(x)$ for "large" x (>1) to the theoretically predicted form (1.9) gives an excellent fit with the parameters F_0 and μ given in Table V. It is reassuring that the value of μ determined here agrees well with the direct numerical determination of μ using (5.17) and from the nonlinear eigenvalue problem discussed in Sec. V. There is a linear regime from about $x=0.2$ to 0.7 where $F(x)$ can be fit to the linear form

$$F(x)=F^{(0)}+F^{(1)}x \tag{6.6}$$

with the parameters shown in Table VI. For $d=2$ the analytic prediction is $F^{(1)}=-0.798$ which agrees reasonably well with the numerical result.

D. Other calculations

Several other numerical calculations have been carried out to check several points. One interesting calculation is to numerically solve the "sharp interface" equation (5.15) directly assuming again initial conditions of the form (4.13). Thus, the calculation n2sl refers to the *non*conserved, *two*-dimensional, *sharp* interface equations solved on the square *lattice*. Another point of interest is the dependence of the results on the underlying lattice. Both of the previous cases were therefore reanalyzed assuming

TABLE III. Numerical fits of $\mu=\frac{1}{2}L^2/t$ to (6.4).

	$\mu^{(0)}$	$\mu^{(-1/2)}$	$\mu^{(-1)}$
n2fl	1.14	1.67	−20.3
n2sl	1.12	1.87	−20.3
n2fi	1.16	0.99	−15.0
n2si	1.11	1.99	−20.2
n3fi	0.58	0.99	−7.52
n3si	0.58	0.75	−5.56

TABLE IV. Numerical fits of $LS_2=A$ to (6.5).

	$A^{(0)}$	$A^{(-1/2)}$	$A^{(-1)}$
n2fl	0.471	0.0236	1.25
n2sl	0.45	0.0071	−1.12
n2fi	0.471	0.0289	−1.29
n2si	0.45	−0.0006	−1.05
n3fi	0.471	0.0069	−1.33
n3si	0.45	−0.0026	−1.3

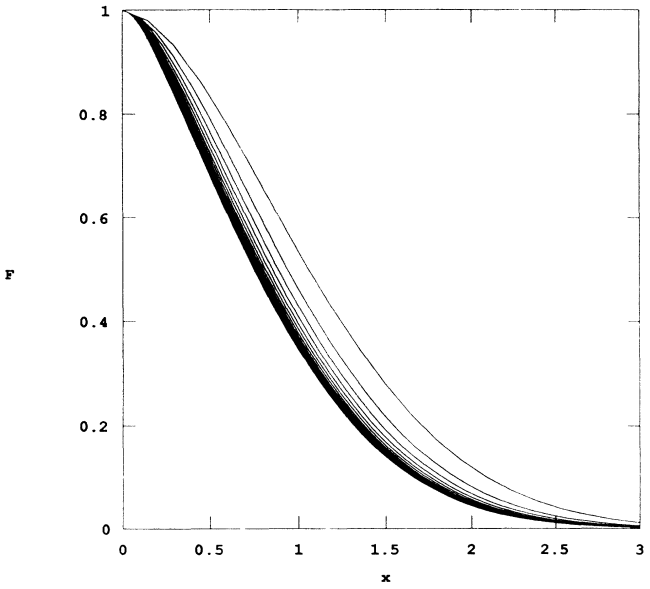

FIG. 4. Scaled structure factor $C(\mathbf{R},t)/C(\mathbf{0},t)$ vs R_x/L (with $L=\sqrt{2}/[1-C(\mathbf{0},t)]$) for various times $t=25$, 50, 75, . . . , 400 after the quench.

the structure factor is isotropic and replacing (6.1) by

$$\nabla_R^2 C(R)=\left[\frac{\partial^2}{\partial R^2}+\frac{(d-1)}{R}\frac{\partial}{\partial R}\right]C(R) \tag{6.7}$$

in d dimensions. The calculations n2fi and n2si therefore reproduce the n2fl and n2sl calculations but with the periodic lattice replaced by an isotropic continuum. Clearly it is straightforward in this case to generalize these calculations to three dimensions. The results of these calculations are given by n3fi and n3si.

The comparison of n2fl and n2sl were carried out for $N=100$. The results shown in Fig. 5 for S or L from the two calculations, as expected, are very different for early times ($t<15$). However, in the range 50–150, the plots for S and L merge. In comparing the structure factors (see Fig. 6) (for $t=400$) one sees that there is excellent agreement for $x>0.8$. In the "linear" regime there is a small, constant discrepancy between the two in the range $0.1<x\leq 0.9$.

In principle, the continuum isotropic limit could be quite different from the lattice model. There is strong evidence however that n2fl and n2fi agree at long times. As shown in Fig. 7, S agrees in detail at long times. Any differences can be ascribed to finite-size differences at long times. The spatial dependence looks quite similar for the two cases. Plots of $F(x)$ shown in Fig. 8 for $t=400$ show close agreement for $x>1$ and reasonably good agreement for small x.

TABLE V. Numerical fits of $F(x)$ to (1.9).

	F_0	μ
n2fl	0.651	1.10
n2sl	0.597	1.10
n2fi	0.591	1.11
n2si	0.608	1.12
n3fi	0.702	0.606
n3si	0.694	0.603

TABLE VI. Numerical fits of $F(x)$ to (6.6).

	$F^{(0)}$	$F^{(1)}$
n2fl	1.06	−0.754
n2sl	1.06	−0.772
n2fi	1.05	−0.762
n2si	1.04	−0.751
n3fi	1.05	−0.547
n3si	1.04	−0.546

The variation of results with the initial conditions were checked for the n2fi system. The cases $S(0)=\epsilon_I=\frac{1}{3}$, 0.274, 0.084 were analyzed and there was *no* dependence of S or S_2 on $S(0)$ at long times.

Fundamentally, as shown in the tables, the long-time structure, including μ, depends only on the dimensionality of the system, not on initial conditions, lattice structure, or on whether one uses the full or sharp interface limit for the driving equations.

VII. SIMULATION

A direct numerical simulation of the original Langevin model with $\lambda=0$ was also carried out. This was accomplished using the same initial conditions given by (4.13) with $\epsilon_I=\frac{1}{3}$. Most of the results were for a 100×100 periodic lattice. The results were averaged over 350 runs. In Fig. 9 the simulation results are compared with the

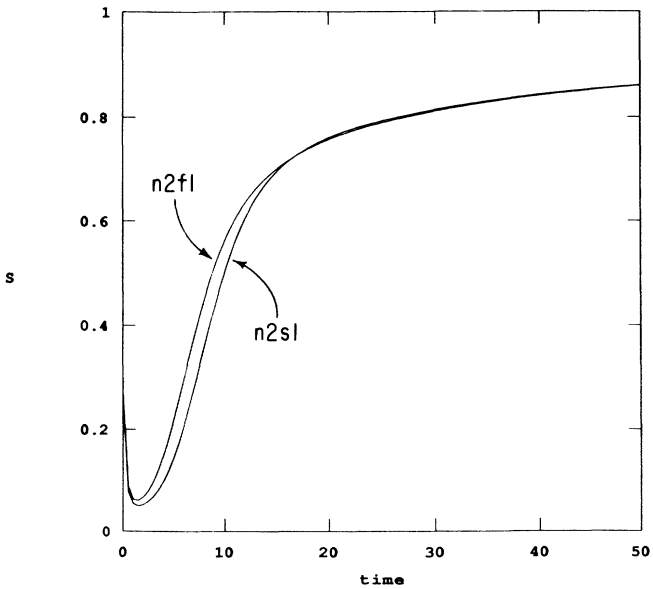

FIG. 5. Comparison of calculations for the full set of equations [defined by (4.11)] and n2fl vs the sharp interface set of equations [defined by (5.15) and n2sl] for $S=C(\mathbf{0},t)$ vs time after the quench.

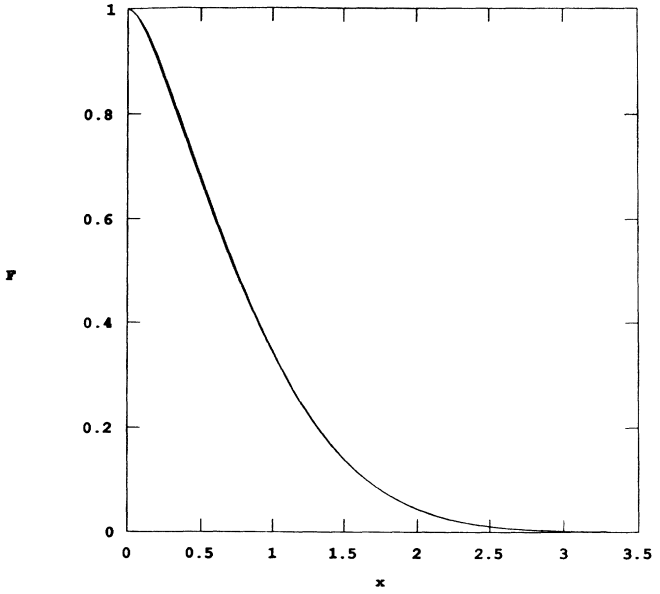

FIG. 6. Same as Fig. 5 but for the scaling function F vs scaled distance $x=R_x/L$.

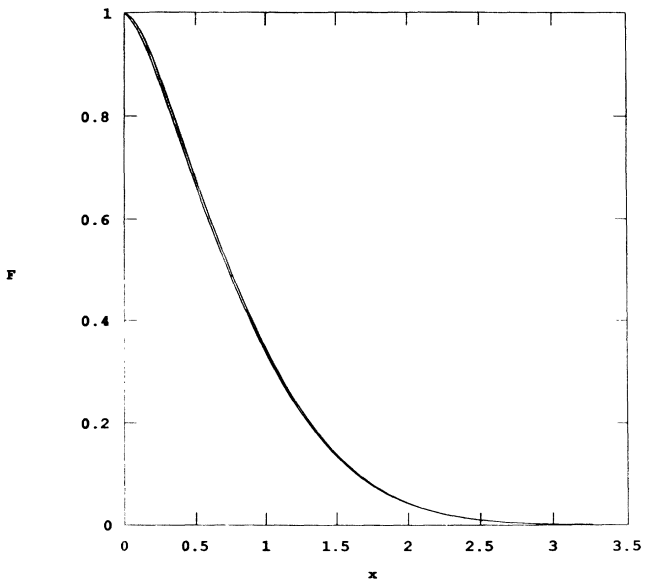

FIG. 8. Same as Fig. 7 but for the scaling function F vs the scaled distance $x=R/L$.

numerical solution of the theory. It can be seen that there is excellent agreement for early and intermediate times. For longer times the simulation lies below the theory and is very well fit by

$$S_{\rm sim}=0.995-1.25\sqrt{t}+0.656/t\ . \tag{7.1}$$

This long-time behavior will be discussed below.

Similarly, the second moment S_2 was determined in the simulation. The result for S_2 from the simulation lies consistently below the result from the theory at long times. However, the quantity LS_2 determined from the simulation can be very well fit to the form

$$LS_2=0.488+0.028/\sqrt{t}-0.734/t\ . \tag{7.2}$$

Comparing this result with the predictions of the theory $LS_2=\sqrt{2}/3=0.471\ldots$ one finds excellent agreement.

The scaling function $F(x)$ has also been determined in the simulation. The comparison with the theory is shown in Fig. 10. The simulation lies consistently above the theoretical result but the overall agreement is quite reasonable since the time ($=100$) for which $F(x)$ was determined is rather modest. Indeed for large x the

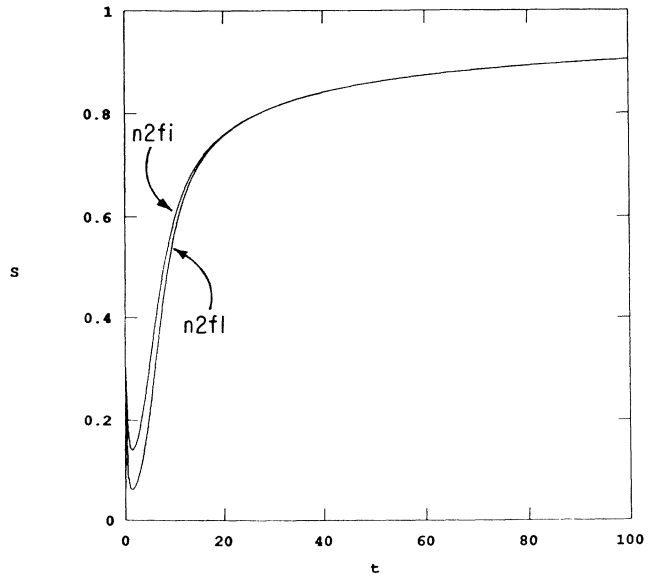

FIG. 7. Comparison of calculations for the full set of equations [defined by (4.11)] set on a lattice (n2fl) or on an isotropic continuum (n2fl).

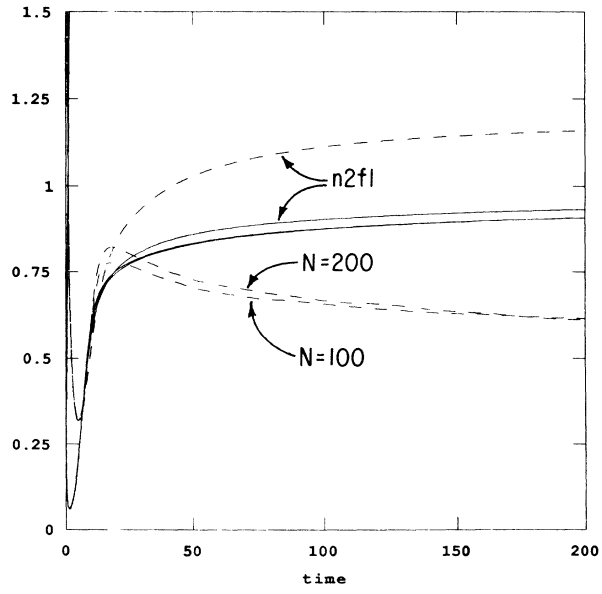

FIG. 9. Simulation results for $N=100$ and 200 and n2fl for μ (dashed curves) and S (solid curves).

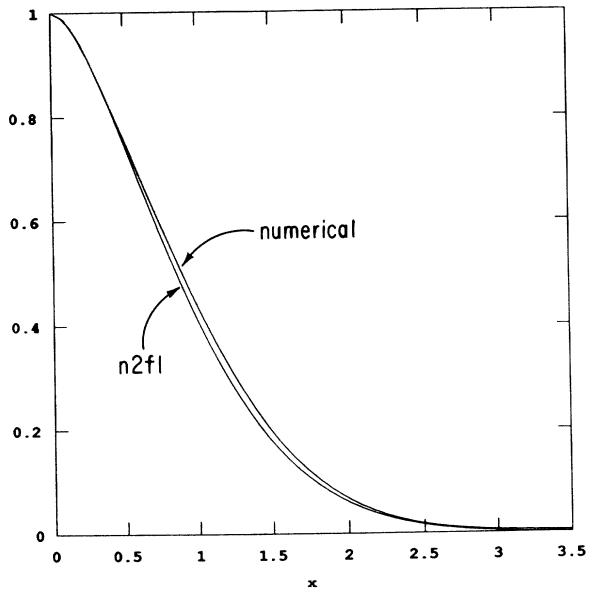

FIG. 10. Simulation results for $N=100$, $t=100$ vs n2fl results for the same parameters for the scaling function F vs scaled distance $x=R_x/L$.

agreement is quite good.

In order to gain some understanding of why there is some discrepancy between the long-time theoretical and simulational results for $S(t)$, it is useful to compare the theoretical results for $\mu=\frac{1}{2}L^2/t$ with those for the simulation. In Fig. 9, μ is shown for the theory and for simulations with $N=100$ and 200. While theory and "experiment" agree for early to intermediate times, there is a definite break at a time of about 20. Clearly the simulations of μ are sensitive to finite-size and boundary effects. μ grows to a larger value for $N=200$ before turning around.

It is possible that $S(t)$ is very sensitive to finite-size effects. For the $N=100$ system there are strong finite-size effects in the tail of $F(x)$ even for $t=100$. Thus, it appears that more careful simulations on much larger systems are necessary to check this point. As was clear in the development of the theory, μ_* can be determined in two ways. One can use $L\dot{L}$ or one can look at the tail of the scaling function and the coefficient in the Gaussian in (1.9). Looking at the simulation one finds for $x>3$, $t=100$, and $N=100$ that the effects of the finite-size and periodic boundary conditions are already substantial in the tail since F is a nonzero (increasing with time) constant in x. This behavior clearly influences the nonlinear matching process described in Sec. V. If, however, one looks directly at the structure factor in the region $2\leq x\leq 2.6$ and fits $F(x)$ to the form (1.9), one obtains $F_0=0.784$ and $\mu=1.05$. The agreement of this value for μ with the theoretical value is encouraging.

VIII. CONCLUSIONS

The theory presented here supports the notion that the scaling properties of growth kinetics are universal. A rather general class of field-theoretical models have been treated and the scaling functions obtained depend only on the spatial dimensionality of the system. Somewhat surprisingly, even the growth law, when measured in units of the equilibrium interfacial width (a quantity which can be rigorously defined), has the universal form (1.5). Whether the fixed-point solution is unstable to yet undiscovered perturbations is an important open question.

It is worthwhile pointing out the range of the results developed here. The growth kinetics of a system described by a single nonconserved scalar order parameter with a degenerate double-well potential with quadratic minima have been treated. For this model the nature of the lattice and the details of the potential are unimportant for the determination of the universal features. It is reasonable to conjecture, as is suggested in MVZ, that nonzero-temperature effects will not change the basic universal features except to replace $\psi_0^2\rightarrow M^2(T)$ and $\xi\rightarrow\xi(T)$, where M and ξ are the temperature-dependent magnetization and interfacial widths which can be computed in equilibrium. One may ask what happens if the field $\psi(\mathbf{R})$ is replaced by fixed-length (Ising) spin. This is an interesting and open question. The answer may be through the mapping of the kinetic Ising model onto a functional integral representation as in Ref. 19.

It is interesting to try and extend these results to other systems. Some extensions are probably simple: the treatment of nonsymmetric degenerate wells or to include higher-order gradients in the equation of motion are obvious checks. From the work of Lai[9] one expects the case of competing scalar order parameters to generate new universality classes. The new element in these cases is the competition between different types of walls and anisotropy.

The most pressing immediate problem of interest is the application of these ideas to the same model but with a conserved order parameter. As indicated in Ref. 7 and in the Introduction, much of the analysis goes through as in the NCOP case. The significant difference is the existence of a long-time competition between the ordering field and the process of bulk diffusion which leads to a crossover from a $t^{1/4}$ to a $t^{1/3}$ growth law. This will be discussed in detail in a companion paper.

The ideas developed here also have application in the problems of front propagation and nucleation. These will be discussed elsewhere.

ACKNOWLEDGMENTS

This work was supported by the National Science Foundation (NSF) Grant No. DMR 88-19860 at The University of Chicago.

[1]K. Binder and D. Stauffer, Phys. Rev. Lett. **33**, 1006 (1974); J. Marro, J. L. Lebowitz, and M. H. Kalos, *ibid.* **43**, 282 (1979); H. Furukawa, Prog. Theor. Phys. **59**, 1072 (1978); Phys. Rev. Lett. **43**, 136 (1979).

[2]For a review, see, J. D. Gunton, M. San Miguel, and P. S. Sahni, in *Phase Transitions and Critical Phenomena*, edited by C. Domb and J. L. Lebowitz (Academic, London, 1983), Vol. 8.

[3]I. M. Lifshitz, Zh. Eksp. Teor. Fiz. **42**, 1354 (1962) [Sov.

Phys.—JETP **15**, 939 (1962)]; S. M. Allen and J. W. Cahn, Acta Metall. **27**, 1085 (1979).

[4]Z. W. Lai, G. F. Mazenko, and O. T. Valls, Phys. Rev. B **37**, 9481 (1988).

[5]S. Kumar, J. D. Gunton, and K. Kaski, Phys. Rev. B **35**, 8517 (1987); J. D. Gunton, E. Gawlinski, A. Chakrabarti, and K. Kaski (unpublished).

[6]A review of earlier theoretical work is given in Ref. 11 and in K. Binder, in *Materials Science and Technology,* Vol. 5 of *Phase Transitions in Materials,* edited by P. Haasen (VCH Verlagsgesellschaft Weinheim, Germany, in press). Among first-principles efforts, the work of J. S. Langer, M. Bar-on, and H. D. Miller, Phys. Rev. A **11**, 1417 (1975) represented the state of the art for a very long time. While MVZ improved this theory in several important ways, it shared with Langer, Bar-on, and Miller (LBM) the deficit of not including sharp interfaces. Reference 7 is the first example, to my knowledge, of a first-principicples theory which does properly include sharp interfaces into the analysis. The very important late-stage interfacial theory developed by K. Kawasaki and T. Ohta, Prog. Theor. Phys. **68**, 129 (1982); T. Ohta, D. Jasnow, and K. Kawasaki, Phys. Rev. Lett. **49**, 1223 (1983); and K. Kawasaki and T. Ohta, Physica (Amsterdam) **118A**, 175 (1983) does not present itself as a first-principles theory. The starting point for this theory assumes an established set of interfaces. The fundamental difference between these theories and that developed here is the existence of a basic equation of motion [Eq. (3.4)] which is valid for all times and which drives the system toward the establishment of a collection of interfaces.

[7]G. F. Mazenko, Phys. Rev. Lett. **63**, 1605 (1989).

[8]G. Porod, in *Small Angle X-Ray Scattering,* edited by O. Glatter and L. Kratky (Academic, New York, 1983).

[9]Z. W. Lai, Phys. Rev. B **41**, 9239 (1990).

[10]S. E. Nagler, Phys. Rev. Lett. **61**, 718 (1988).

[11]G. F. Mazenko, O. T. Valls, and M. Zannetti, Phys. Rev. B **38**, 520 (1988).

[12]G. F. Mazenko, O. T. Valls, and M. Zannetti, Phys. Rev. B **40**, 3676 (1989).

[13]This first argument was presented to me by Professor P. Nozieres.

[14]H. Tomita, Prog. Theor. Phys. **72**, 656 (1984); **75**, 482 (1986).

[15]A useful discussion is given by Y. Ono and S. Puri, Mod. Phys. Lett. **2**, 861 (1988).

[16]P. C. Martin, E. D. Siggia, and H. A. Rose, Phys. Rev. A **8**, 423 (1973).

[17]C. de Dominicis and L. Peliti, Rev. B **18**, 353 (1978).

[18]E. Brezin, J. C. LeGuillou, and J. Zinn-Justin, in *Phase Transitions and Critical Phenomena,* edited by C. Domb and M. Green (Academic, London, 1976), Vol. 6.

[19]H. Sommers, Phys. Rev. Lett. **58**, 1268 (1987).